

GW170817: Measurements of Neutron Star Radii and Equation of State

The LIGO Scientific Collaboration and The Virgo Collaboration

On 17 August 2017, the LIGO and Virgo observatories made the first direct detection of gravitational waves from the coalescence of a neutron star binary system. The detection of this gravitational-wave signal, GW170817, offers a novel opportunity to directly probe the properties of matter at the extreme conditions found in the interior of these stars. The initial, minimal-assumption analysis of the LIGO and Virgo data placed constraints on the tidal effects of the coalescing bodies, which were then translated to constraints on neutron star radii. Here, we expand upon previous analyses by working under the hypothesis that both bodies were neutron stars that are described by the same equation of state and have spins within the range observed in Galactic binary neutron stars. Our analysis employs two methods: the use of equation-of-state-insensitive relations between various macroscopic properties of the neutron stars and the use of an efficient parametrization of the defining function $p(\rho)$ of the equation of state itself. From the LIGO and Virgo data alone and the first method, we measure the two neutron star radii as $R_1 = 10.8^{+2.0}_{-1.7}$ km for the heavier star and $R_2 = 10.7^{+2.1}_{-1.5}$ km for the lighter star at the 90% credible level. If we additionally require that the equation of state supports neutron stars with masses larger than $1.97 M_\odot$ as required from electromagnetic observations and employ the equation-of-state parametrization, we further constrain $R_1 = 11.9^{+1.4}_{-1.4}$ km and $R_2 = 11.9^{+1.4}_{-1.4}$ km at the 90% credible level. Finally, we obtain constraints on $p(\rho)$ at supranuclear densities, with pressure at twice nuclear saturation density measured at $3.5^{+2.7}_{-1.7} \times 10^{34}$ dyn cm⁻² at the 90% level.

INTRODUCTION

Since September 2015, the Advanced LIGO [1] and Advanced Virgo [2] observatories have opened a window on the gravitational-wave (GW) universe [3, 4]. A new type of astrophysical source of GWs was detected on 17 August 2017, when the GW signal emitted by a low-mass coalescing compact binary was observed [5]. This observation coincided with the detection of a γ -ray burst, GRB 170817A [6, 7], verifying that the source binary contained matter, which was further corroborated by a series of observations that followed across the electromagnetic spectrum; see e.g. [8–12]. The measured masses of the bodies and the variety of electromagnetic observations are consistent with neutron stars (NSs).

Neutron stars are unique natural laboratories for studying the behavior of cold high-density nuclear matter. Such behavior is governed by the equation of state (EOS), which prescribes a relationship between pressure and density. This determines the relation between NS mass and radius, as well as other macroscopic properties such as the stellar moment of inertia and the tidal deformability (see e.g. [13]). While terrestrial experiments are able to test and constrain the cold EOS at densities below and near the saturation density of nuclei $\rho_{\text{nuc}} = 2.8 \times 10^{14}$ g cm⁻³ (see e.g. [14–17] for a review), currently they cannot probe the extreme conditions in the deep core of NSs. Astrophysical measurements of NS masses, radii, moments of inertia and tidal effects, on the other hand, have the potential to offer information about whether the EOS is soft or stiff and what the pressure is at several times the nuclear saturation density [16, 18–20].

GWs offer an opportunity for such astrophysical measurements to be performed, as the GW signal emitted by

merging NS binaries differs from that of two merging black holes (BHs). The most prominent effect of matter during the observed binary inspiral comes from the tidal deformation that each star’s gravitational field induces on its companion. This deformation enhances GW emission and thus accelerates the decay of the quasicircular inspiral [21–23]. In the post-Newtonian (PN) expansion of the inspiral dynamics [24–32], this effect causes the phase of the GW signal to differ from that of a binary BH (BBH) from the fifth PN order onwards [21, 33, 34]. The leading-order contribution is proportional to each star’s tidal deformability parameter, $\Lambda = (2/3)k_2 C^{-5}$, an EOS-sensitive quantity that describes how much a star is deformed in the presence of a tidal field. Here k_2 is the $l = 2$ relativistic Love number [35–39], $C \equiv Gm/(c^2 R)$ is the compactness, R is the areal radius, and m is the mass of the NS. The deformation of each NS due to its own spin also modifies the waveform and depends on the EOS. This effect enters the post-Newtonian expansion as a contribution to the (lowest order) spin-spin term at the second order in the GW phase [40, 41]. The EOS also affects the waveform at merger, the merger outcome and its lifetime, as well as the postmerger emission (see e.g. [42]). Finally, other stellar modes can couple to the tidal field and affect the GW signal [21, 43–45].

Among the various EOS-dependent effects, the tidal deformation is the one most readily measurable with GW170817. The spin-induced quadrupole has a larger effect on the orbital evolution for systems with large NS spin [46–49] but is also largely degenerate with the mass ratio and the NS spins, making it difficult to measure independently [50]. The postmerger signal, while rich in content, is also difficult to observe, with current detector sensitivities being limited due to photon shot noise [1] at the high frequencies of interest. The merger and postmerger

signal make a negligible contribution to our inference for GW170817 [51, 52].

In [5], we presented the first measurements of the properties of GW170817, including a first set of constraints on the tidal deformabilities of the two compact objects, from which inferences about the EOS can be made. An independent analysis further exploring how well the gravitational-wave data can be used to constrain the tidal deformabilities, and, from that, the NS radii, has also been performed recently [53]. Our initial bounds have facilitated a large number of studies, e.g. [54–64], aiming to translate the measurements of masses and tidal deformabilities into constraints on the EOS of NS matter. In a companion paper [52], we perform a more detailed analysis focusing on the source properties, improving upon the original analysis of [5] by using Virgo data with reduced calibration uncertainty, extending the analysis to lower frequencies, employing more accurate waveform models, and fixing the location of the source in the sky to the one identified by the electromagnetic observations.

Here we complement the analysis of [52], and work under the hypothesis that GW170817 was the result of a coalescence of two NSs whose masses and spins are consistent with astrophysical observations and expectations. Moreover since NSs represent equilibrium ground-state configurations, we assume that their properties are described by the same EOS. By making these additional assumptions, we are able to further improve our measurements of the tidal deformabilities of GW170817, and constrain the radii of the two NSs. Moreover, we use an efficient parametrization of the EOS to place constraints on the pressure of cold matter at supranuclear densities using GW observations. This direct measurement of the pressure takes into account physical and observational constraints on the NS EOS, namely causality, thermodynamic stability, and a lower limit on the maximum NS mass supported by the EOS to be $M_{\text{max}} > 1.97 M_{\odot}$. The latter is chosen as a 1σ conservative estimate, based on the observation of PSR J0348+0432 with $M = 2.01 \pm 0.04 M_{\odot}$ [65], the heaviest NS known to date.

The radii measurements presented here improve upon existing results (e.g. [58, 62]) which had used the initial tidal measurements reported in [5]. We also verify that our radii measurements are consistent with the result of the methodologies presented in these studies when applied to our improved tidal measurements. Moreover, we obtain a more precise estimate of the NS radius than [53].

METHODS

In this section we describe the details of the analysis. We use the same LIGO and Virgo data and calibration model analyzed in [52]. The data can be downloaded from the Gravitational Wave Open Science Center (GWOSC) [66]. The data include the subtraction of an instrumental artifact

occurring at LIGO-Livingston within 2 s of the GW170817 merger [5, 67], as well as the subtraction of independently measurable noise sources [68–71].

Bayesian methods

We employ a coherent Bayesian analysis to estimate the source parameters $\vec{\vartheta}$ as described in [72, 73]. The goal is to determine the posterior probability density function (PDF), $p(\vec{\vartheta}|d)$, given the LIGO and Virgo data d . Given a prior PDF $p(\vec{\vartheta})$ on the parameter space (quantifying our prior belief in observing a source with properties $\vec{\vartheta}$), the posterior PDF is given by Bayes’s theorem $p(\vec{\vartheta}|d) \propto p(\vec{\vartheta})p(d|\vec{\vartheta})$, where $p(d|\vec{\vartheta})$ is the likelihood of obtaining the data d given that a signal with parameters $\vec{\vartheta}$ is present in the data. Evaluating the multidimensional $p(\vec{\vartheta}|d)$ analytically is computationally prohibitive so we resort to sampling techniques to efficiently draw samples from the underlying distribution. We make use of the Markov-chain Monte Carlo algorithm as implemented in the LALINFERENCE package [72], which is part of the publicly available LSC Algorithm Library (LAL) [74]. For the likelihood calculation, we use 128 s of data around GW170817 over a frequency range of 23–2048 Hz, covering both the time and frequency ranges where there was appreciable signal above the detector noise, and we estimate the likelihood for our waveform templates up to merger. The power spectral density (PSD) of the noise is computed on source [52, 75, 76], and we marginalize over the detectors’ calibration uncertainties as described in [52, 73, 77].

In the analysis of a GW signal from a binary NS coalescence, the source parameters $\vec{\vartheta}$ on which the signal depends can be decomposed as $\vec{\vartheta} = (\vec{\vartheta}_{\text{PM}}, \vec{\vartheta}_{\text{EOS}})$, into parameters that would be present if the two bodies behaved like point masses $\vec{\vartheta}_{\text{PM}}$, and EOS-sensitive parameters $\vec{\vartheta}_{\text{EOS}}$ that arise due to matter effects of the two finite-sized bodies (e.g. tidal deformabilities). The priors on the point-mass parameters that we use are described in Sec. II D of [52] and we do not repeat them here. We also use the same convention for the component masses, i.e. $m_1 \geq m_2$. We only consider the “low-spin” prior of [52] where the dimensionless NS spin parameter is restricted to $\chi \leq 0.05$, in agreement with expectations from Galactic binary NS spin measurements [78], and we fix the location of the source in the sky to the one given by EM observations. Regarding the EOS-related part of the parameter space and the corresponding priors, we consider two physically motivated parameterizations of different dimensionalities, which we describe in detail in the following sections. The first method requires the sampling of tidal deformability parameters, whereas the second method directly samples the EOS function $p(\rho)$ from a 4-dimensional family of functions. In both cases, the assumption that the binary consists of two NSs that are

described by the same EOS is implicit in the parametrization of matter effects (in contrast with the analysis of [52], where minimal assumptions are made about the nature of the source).

Waveform models and matter effects

The measurement process described above requires a waveform model that maps the source parameters $\vec{\vartheta}$ to a signal $h(t; \vec{\vartheta})$ that would be observed in the detector. The publicly available LALSIMULATION software package of LAL [74] contains several such waveform models obtained with different theoretical approaches. The impact of varying the models among several choices [21, 22, 41, 79–94] is analyzed in detail in [52], showing that for GW170817 the systematic uncertainties due to the modeling of matter effects or the underlying point-particle description are smaller than the statistical errors in the measurement. We perform a similar analysis here by varying the BBH baseline model or using a post-Newtonian waveform prescription and find results consistent with those presented in Sec. III D and Table IV of [52]. Moreover, the study of Appendix A of [52] (Table V) suggests that varying the tidal description in the waveforms also leads to broadly consistent tidal measurements. Since the net effect of varying waveform models is very different for each of the source properties, we refer to the tables and figures in [52] for quantitative statements to assess the impact of modeling uncertainties.

In the GW170817 discovery paper [5] the results for the inferred tidal deformabilities were obtained with the TaylorF2 model that is based solely on post-Newtonian results for both the BBH baseline model [41, 90–94] and for tidal effects [21, 22], as this model led to the conservatively largest bounds. In this Letter, we use a more realistic waveform model PhenomPNRT [79–83], which is also used as the reference model in our detailed analysis of the properties of GW170817 [52]. The BBH baseline in this model, constructed based on [24, 91–93, 95–98], is calibrated to numerical relativity data and describes relativistic point-mass, spin, and the dominant precession effects. The model further includes tidal effects in the phase from combining analytical information [22, 23, 86, 99] with results from numerical-relativity simulations of binary NSs as described in [84, 100], and matter effects in the spin-induced quadrupole based post-Newtonian results [40, 41, 92–94]. The characteristic rotational quadrupole deformation parameters are computed from Λ through EOS-insensitive relations [101, 102] as described in [48, 103]. Other matter effects with nonzero spins are not taken into account in our analysis.

EOS-insensitive relations

Despite the microscopic complexity of NSs, some of their macroscopic properties are linked by EOS-insensitive relations that depend only weakly on the EOS [104]. We use two such relations to ensure that the two NSs obey the same EOS and to translate NS tidal deformabilities to NS radii.

The first such relation we employ was constructed in [105] and studied in the context of realistic GW inference in [106]. It combines the mass ratio of the binary $q \equiv m_2/m_1 \leq 1$, the symmetric tidal deformability $\Lambda_s \equiv (\Lambda_2 + \Lambda_1)/2$ and the antisymmetric tidal deformability $\Lambda_a \equiv (\Lambda_2 - \Lambda_1)/2$ in a relation of the form $\Lambda_a(\Lambda_s, q)$. Fitting coefficients and an estimate of the relation’s intrinsic error were obtained by tuning to a large set of EOS models [104, 106], ensuring that the relation gives pairs of tidal deformabilities that correspond to realistic EOS models. We sample uniformly in the symmetric tidal deformability $\Lambda_s \in [0, 5000]$, use the EOS-insensitive relation to compute Λ_a , and then obtain Λ_1 and Λ_2 , which are used to generate a waveform template. The sampling of tidal parameters also involves a marginalization over the intrinsic error in the relation, which is also a function of Λ_s and q . This procedure leads to unbiased estimation of the tidal parameters for a wide range of EOSs and mass ratios [106].

The second relation we employ is between NS tidal deformability Λ and NS compactness C [107, 108]. We employ this Λ – C relation with the coefficients given in Sec. (4.4) of [104] to compute the posterior for the radius and the mass of each binary component. Reference [104] reports a maximum 6.5% relative error in the relation when compared to a large set of EOS models. We assume that the relative error is constant across the parameter space and distributed according to a zero-mean Gaussian with a standard deviation of $(6.5/3)\%$ and marginalize over it. We verified that our results are not sensitive to this choice of error estimate by comparing to the more conservative choice of a uniform distribution in $[-6.5\%, 6.5\%]$.

Parametrized EOS

Instead of sampling macroscopic EOS-related parameters such as tidal deformabilities, one may instead sample the defining function $p(\rho)$ of the EOS directly. A number of parametrizations of different degrees of complexity and fidelity to realistic EOS models have been proposed (see [109] for a review), and here we employ the spectral parametrization constructed and validated in [110–112]. This parametrization expresses the logarithm of the adiabatic index of the EOS $\Gamma(p; \gamma_i)$, as a polynomial of the pressure p , where $\gamma_i = (\gamma_0, \gamma_1, \gamma_2, \gamma_3)$ are the free EOS parameters. The adiabatic index is then used to compute the energy $\epsilon(p; \gamma_i)$ and rest-mass density $\rho(p; \gamma_i)$, which are inverted to give the EOS. The parameterized

high-density EOS is then stitched to the SLy EOS [113] below about half the nuclear saturation density. This is chosen because such low densities do not significantly impact the global properties of the NS [114]. Different low density EOSs can produce a difference in radius, for a given m , of order 0.1 km. Though use of a specific parametrization makes our results model-dependent, we have checked that they are consistent with another common EOS parametrization, the piecewise polytropic one [115, 116], as also found in [117].

In this analysis, we follow the methodology detailed in [117], developed from the work of [118], to sample directly in an EOS parameter space. We sample uniformly in all EOS parameters within the following ranges: $\gamma_0 \in [0.2, 2]$, $\gamma_1 \in [-1.6, 1.7]$, $\gamma_2 \in [-0.6, 0.6]$, and $\gamma_3 \in [-0.02, 0.02]$ and additionally impose that the adiabatic index $\Gamma(p) \in [0.6, 4.5]$. This choice of prior ranges for the EOS parameters was chosen such that our parametrization encompasses a wide range of candidate EOSs [110] and leads to NSs with a compactness below 0.33 and a tidal deformability above about 10. Then for each sample, the four EOS parameters and the masses are mapped to a (Λ_1, Λ_2) pair through the Tolman-Oppenheimer-Volkoff (TOV) equations describing the equilibrium configuration of a spherical star [119]. The two tidal deformabilities are then used to compute the waveform template.

Sampling directly in the EOS parameter space allows for certain prior constraints to be conveniently incorporated in the analysis. In our analysis, we impose the following criteria on all EOS and mass samples: (i) causality, the speed of sound in the NS ($\sqrt{dp/d\epsilon}$) must be less than the speed of light (plus 10% to allow for imperfect parametrization) up to the central pressure of the heaviest star supported by the EOS; (ii) internal consistency, the EOS must support the proposed masses of each component; and (iii) observational consistency, the EOS must have a maximum mass at least as high as previously observed NS masses, specifically $1.97 M_\odot$. Another condition the EOS must obey is that of thermodynamic stability; the EOS must be monotonically increasing ($d\epsilon/dp > 0$). This condition is built into the parametrization [110], so we do not need to explicitly impose it.

RESULTS

We begin by demonstrating the improvement in the measurement of the tidal deformability parameters due to imposing a common but unknown EOS for the two NSs. In Fig. 1 we show the marginalized joint posterior PDF for the individual tidal deformabilities. We show results from our analysis using the $\Lambda_a(\Lambda_s, q)$ relation in green and the parametrized EOS without a maximum mass constraint in blue. These are compared to results from [52], where the two tidal deformability parameters are sampled independently, in orange. The shaded region marks the $\Lambda_2 < \Lambda_1$

region that is naturally excluded when a common realistic EOS is assumed, but is not excluded from the analysis of [52]. In both cases imposing a common EOS leads to a smaller uncertainty in the tidal deformability measurement. The area of the 90% credible region for the Λ_1 - Λ_2 posterior shrinks by a factor of ~ 3 , which is consistent with the results of [106] for soft EOSs and NSs with similar masses. The tidal deformability of a $1.4 M_\odot$ NS can be estimated through a linear expansion of $\Lambda(m)m^5$ around $1.4 M_\odot$ as in [5, 48, 120] to be $\Lambda_{1.4} = 190^{+390}_{-120}$ at the 90% level when a common EOS is imposed (here and throughout this paper we quote symmetric credible intervals). Our results suggest that “soft” EOSs such as APR4, which predict smaller values of the tidal deformability parameter, are favored over “stiff” EOSs such as H4 or MS1, which predict larger values of the tidal deformability parameter and lie outside the 90% credible region.

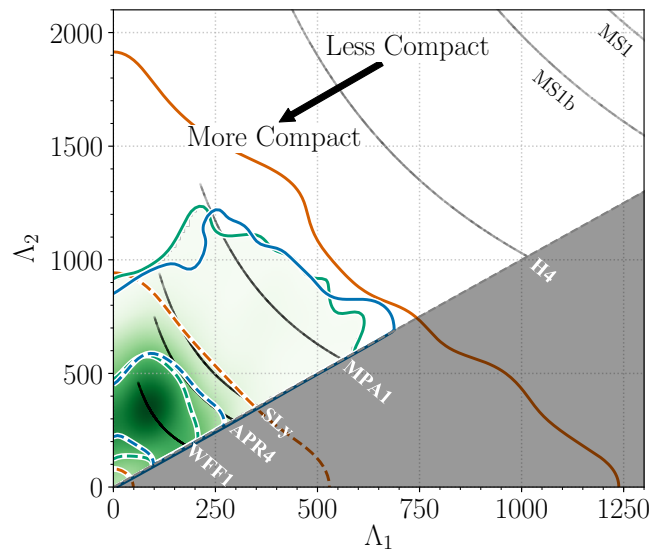


FIG. 1. Marginalized posterior for the tidal deformabilities of the two binary components of GW170817. The green shading shows the posterior obtained using the $\Lambda_a(\Lambda_s, q)$ EOS-insensitive relation to impose a common EOS for the two bodies, while the green, blue, and orange lines denote 50% (dashed) and 90% (solid) credible levels for the posteriors obtained using EOS-insensitive relations, a parametrized EOS without a maximum mass requirement, and independent EOSs (taken from [52]), respectively. The gray shading corresponds to the unphysical region $\Lambda_2 < \Lambda_1$ while the seven black scatter regions give the tidal parameters predicted by characteristic EOS models for this event [113, 115, 121–125].

We next explore what inferences we can make about the structure of NSs. We do this using the spectral EOS parametrization described above in combination with the requirement that the EOS must support NSs up to at least $1.97 M_\odot$, a conservative estimate based on the heaviest known pulsar [65]. From this we obtain a posterior for the NS interior pressure as a function of rest-mass density. The

result is shown in Fig. 2, along with marginalized posteriors for central densities and central pressures and predictions of the pressure-density relationship from various EOS models. The pressure posterior is shifted from the 90% credible prior region (marked by the purple dashed lines) and towards the soft floor of the parametrized family of EOS. This means that the posterior is indicating more support for softer EOS than the prior. The solid vertical lines denote the nuclear saturation density and two more rest-mass density values that are known to approximately correlate with bulk macroscopic properties of NSs [19]. The pressure at twice (six times) the nuclear saturation density is measured to be $3.5_{-1.7}^{+2.7} \times 10^{34}$ ($9.0_{-2.6}^{+7.9} \times 10^{35}$) dyn/cm² at the 90% level.

The pressure posterior appears to show minor signs of a bend above a density of $\sim 5\rho_{\text{nuc}}$. Evidence of such behavior at high densities would be an indication of extra degrees of freedom, though this is not an outcome of the GW data alone. Indeed in the top (right) panel, the vertical (horizontal) lines denote the 90% confidence intervals for the central densities (pressures) of the two stars, suggesting that our data are not informative for densities (pressures) above those intervals. The bend is an outcome of two competing effects: the GW data point toward a lower pressure, while the requirement that the EOS supports masses above $1.97 M_{\odot}$ demands a high pressure at large densities. The result is a precise pressure estimate at around $5\rho_{\text{nuc}}$ and a broadening above that, giving the impression of a bend in the pressure. We have verified that the bend is absent if we remove the maximum mass constraint from our analysis.

Finally we place constraints in the 2-dimensional parameter space of the NS mass and areal radius for each binary component. This posterior is shown in Fig. 3. The left panel is obtained by first using the $\Lambda_a(\Lambda_s, q)$ relation to obtain tidal deformability samples assuming a common EOS and then using the Λ - C relation to compute the NS radii. The right panel is computed by integrating the TOV equation to compute the radius for each sample in the spectral EOS parametrization after imposing a maximum mass of at least $1.97 M_{\odot}$. At the 90% level, the radii of the two NSs are $R_1 = 10.8_{-1.7}^{+2.0}$ km and $R_2 = 10.7_{-1.5}^{+2.1}$ km from the left panel and $R_1 = 11.9_{-1.4}^{+1.4}$ km and $R_2 = 11.9_{-1.4}^{+1.4}$ km from the right panel. The one-sided 90% lower [upper] limit on $m_2[m_1]$ is $(1.15, 1.36)M_{\odot}$ [$(1.36, 1.62)M_{\odot}$] from the left panel and $(1.18, 1.36)M_{\odot}$ [$(1.36, 1.58)M_{\odot}$] from the right panel, consistent with the results of Ref. [52]. We note that the Λ - C relation has not been established to values of Λ less than 20 [104]. In order to check the validity of our EOS-insensitive results in this regime, we first verify that the parametrized-EOS results without a maximum mass constraint satisfy the Λ - C relation to the required accuracy, even for $\Lambda_1 < 20$. Furthermore, we find that our radius and mass estimates are unaffected if we discard all $\Lambda_1 < 10$ samples.

The difference between the two radius estimates is mainly due to different physical information included in

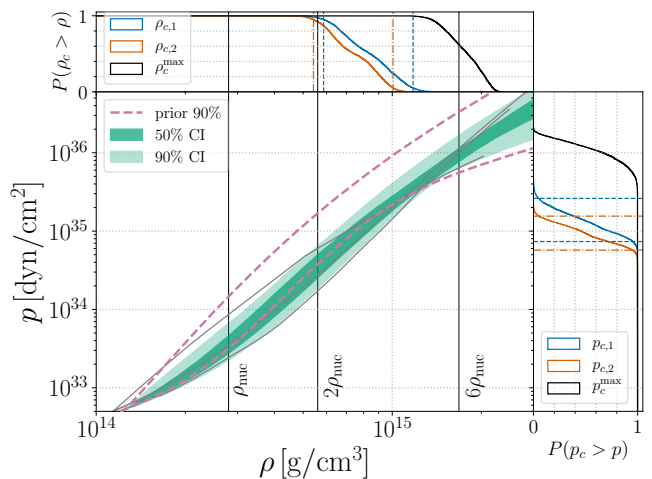


FIG. 2. Marginalized posterior (green bands) and prior (purple dashed) for the pressure p as a function of the rest-mass density ρ of the NS interior using the spectral EOS parametrization and imposing a lower limit on the maximum NS mass supported by the EOS of $1.97 M_{\odot}$. The dark (light) shaded region corresponds to the 50% (90%) posterior credible level and the purple dashed lines show the 90% prior credible interval. Vertical lines correspond to once, twice, and six times the nuclear saturation density. Overplotted in gray are representative EOS models [121, 122, 124], using data taken from [19]; from top to bottom at $2\rho_{\text{nuc}}$ we show H4, APR4, and WFF1. The corner plots show cumulative posteriors of central densities ρ_c (top) and central pressures p_c (right) for the two NSs (blue and orange), as well as for the heaviest NS that the EOS supports (black). The 90% credible intervals for ρ_c and p_c are denoted by vertical and horizontal lines respectively for the heavier (blue dashed) and lighter (orange dot-dashed) NS.

each analysis. The EOS-insensitive-relations analysis (left panel) is based on GW data alone, while the parametrized-EOS analysis (right panel) imposes an additional observational constraint, namely that the EOS must support NSs of at least $1.97 M_{\odot}$. This has a large effect on the radii priors as shown in the 1-dimensional plots of Fig. 3, since small radii are typically predicted by soft EOSs, which cannot support large NS masses. In the case of EOS-insensitive relations (left panel), the prior allows for smaller values of the radius than in the parametrized-EOS case (right panel), something that is reflected in the posteriors since the GW data alone cannot rule out radii below ~ 10 km. Therefore the lower radius limit in the EOS-insensitive-relations analysis is determined by the GW measurement, while in the case of the parametrized-EOS analysis it is determined by the mass of the heaviest observed pulsar and its implications for NS radii [65]. Additionally, we verified that the parametrized-EOS analysis without the maximum mass constraint leads to similar results to the EOS-insensitive-relations analysis.

To quantify the improvement from assuming that both NSs obey the same EOS, we apply the Λ - C relation to

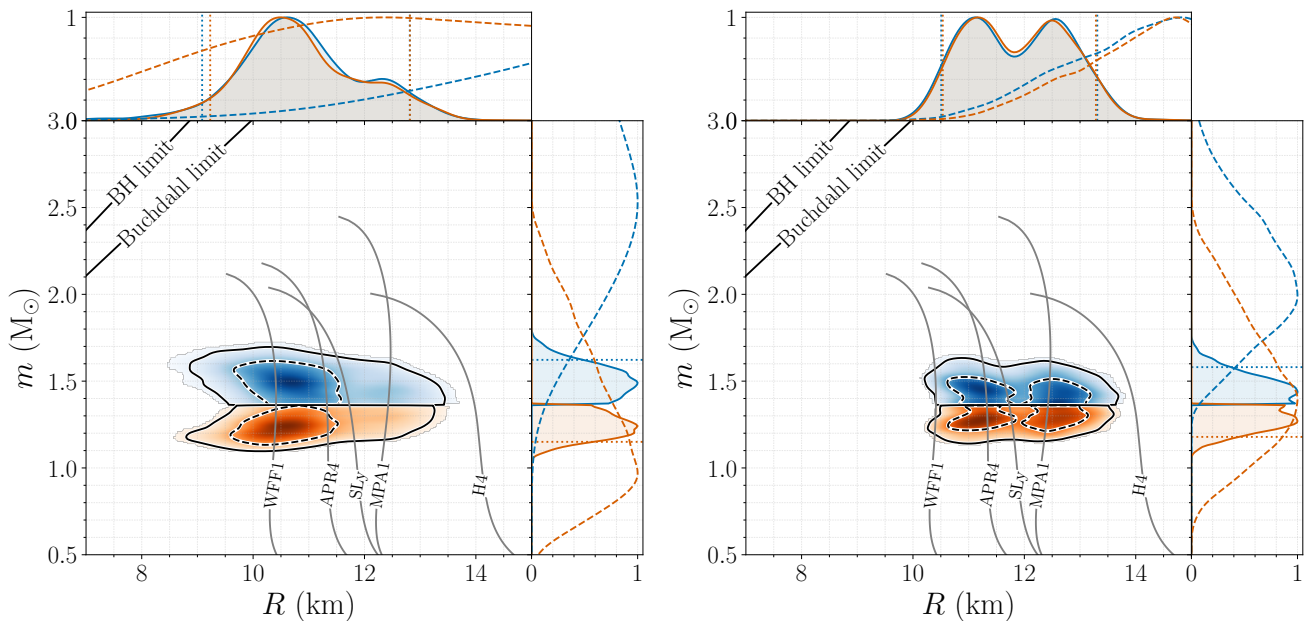


FIG. 3. Marginalized posterior for the mass m and areal radius R of each binary component using EOS-insensitive relations (left panel) and a parametrized EOS where we impose a lower limit on the maximum mass of $1.97 M_{\odot}$ (right panel). The top blue (bottom orange) posterior corresponds to the heavier (lighter) NS. Example mass-radius curves for selected EOSs are overplotted in gray. The lines in the top left denote the Schwarzschild BH ($R = 2m$) and Buchdahl ($R = 9m/4$) limits. In the one-dimensional plots, solid lines are used for the posteriors, while dashed lines are used for the corresponding parameter priors. Dotted vertical lines are used for the bounds of the 90% credible intervals.

tidal deformability samples calculated without assuming the $\Lambda_a(\Lambda_s, q)$ relation (the orange posterior of Fig. 1) and obtain $R_1 = 11.8_{-3.3}^{+2.7}$ km and $R_2 = 10.8_{-3.0}^{+2.9}$ km at the 90% level. This suggests that imposing a common EOS for the two binary components leads to a reduction of the 90% credible interval width for the radius measurement of almost a factor of 2, from 5.9 to 3.6 km.

DISCUSSION

In this Letter, we complement our analysis of the tidal effects of GW170817 in [52] with a targeted analysis that assumes astrophysically plausible NS spins and tidal parameters, as well as the same EOS for both NSs. This additional prior information enables us to measure NS radii with an uncertainty less than 2.8 km if consistency with observed pulsar masses is enforced, and 3.6 km using GW data alone at the 90% credible level. We observe that, in both cases, the data are informative and drive the upper bounds on the NS radii and the stiffness of the EOS. Simultaneously, the pressure at twice the nuclear saturation density is measured to be $p(2\rho_{\text{nuc}}) = 3.5_{-1.7}^{+2.7} \times 10^{34}$ dyn/cm². Our results are consistent with x-ray binary observations (see, e.g. [19, 20, 126, 127]) and suggest that NS radii are not large. Additionally, our results can be compared to tidal inference based on the electromagnetic emission of GW170817 [128–130].

Our results are comparable and consistent with studies that use the tidal measurement from [5] to obtain bounds on NS radii. Using our bound of $\Lambda_{1.4} < 800$ (the only tidal parameter in [5], which assumed a common EOS for both NSs) and different EOS parametrizations, several studies found $R_{1.4} \lesssim 13.5$ km [56, 58, 62, 64]. Reference [63] arrives at a similar conclusion using our $\tilde{\Lambda} < 800$ constraint [5] (though see [52] for an amended $\tilde{\Lambda}$ bound) and the observation that $\tilde{\Lambda}$ is almost insensitive to the binary mass ratio [99]. Our improved estimate of $\Lambda_{1.4} = 190_{-120}^{+390}$, and $R_1 = 10.8_{-1.7}^{+2.0}$ km and $R_2 = 10.7_{-1.5}^{+2.1}$ km for the EOS-insensitive-relation analysis is roughly consistent with these estimates (see for example Fig. 1 of [62] and [58]). If we additionally enforce the heaviest observed pulsar to be supported by placing direct constraints on the EOS parameter space, we get further improvement in the radius measurement, with $R_1 = 11.9_{-1.4}^{+1.4}$ km and $R_2 = 11.9_{-1.4}^{+1.4}$ km.

A recent analysis of the GW170817 data was performed in De *et al.* [53] using the TaylorF2 model, imposing that the two NSs have the same radii which, under the additional assumption that $\Lambda \propto C^{-6}$ (an alternative to the Λ – C relation used here [104]), directly relates the two tidal deformabilities as $\Lambda_1 = q^6 \Lambda_2$. After our paper appeared as a preprint, De *et al.* obtained a revised estimate of the common NS radius $8.9 \text{ km} < \hat{R} < 13.2 \text{ km}$. Despite using a lower low-frequency cutoff – and hence more data

– than our study, the result of De *et al.* corresponds to a width of 4.3 km, which is wider than the uncertainty on radii computed under our EOS-insensitive analysis. There are differences in several details of the setup of the two analyses (most notably, frequency range, data calibration, the noise PSD estimation, waveform model, parameter priors, assumed relations between radii and Λ s and treatment of corresponding uncertainties), each of which may be responsible for part of the observed discrepancies.

Our results, and specifically the lower radius limit, do not constitute observational proof of tidal effects in GW170817, as our analysis has explicitly assumed that the coalescing bodies were NSs both in terms of their spins and tidal deformabilities. In particular, the spins are restricted to small values typical for galactic NSs in binaries, and the tidal deformabilities are calculated consistently assuming a common typical NS EOS. Moreover, the Λ – C map diverges as Λ approaches zero (BH), and therefore the lower bounds obtained for the radii do not imply lower bounds on the tidal deformabilities. Meanwhile, the analysis of [52] assumes independent tidal parameters and finds a lower bound on $\tilde{\Lambda}$ only under the small-spin assumption but not if spins larger than 0.05 are allowed.

The detection of GW170817 has opened new avenues in astrophysics and in the study of matter at conditions currently unattainable in terrestrial laboratories. As the network of GW observatories expands and improves in sensitivity, we expect many more observations of BNS mergers [4]. Each new observation will yield additional information about the properties of NSs, and the increasing precision of our measurements will simultaneously raise new challenges. As statistical uncertainties shrink, systematic uncertainties that are naturally introduced by our models and the underlying assumptions of our methods may begin to dominate. Improved waveform models and data analysis techniques are an area of active research for the GW community, and will be required to achieve our most complete understanding of these extreme systems.

Data associated with the figures in this article, including posterior samples generated using the PhenomPNRT model, can be found at dcc.ligo.org/LIGO-P1800115/public. The GW strain data for this event are available at the Gravitational Wave Open Science Center [131]. This article has been assigned the document number ligo-p1800115.

ACKNOWLEDGMENTS

The authors gratefully acknowledge the support of the U.S. National Science Foundation (NSF) for the construction and operation of the LIGO Laboratory and Advanced LIGO as well as the Science and Technology Facilities Council (STFC) of the United Kingdom, the Max-Planck-Society (MPS), and the State of Niedersachsen/Germany for support of the construction of Advanced LIGO and

construction and operation of the GEO600 detector. Additional support for Advanced LIGO was provided by the Australian Research Council. The authors gratefully acknowledge the Italian Istituto Nazionale di Fisica Nucleare (INFN), the French Centre National de la Recherche Scientifique (CNRS) and the Foundation for Fundamental Research on Matter supported by the Netherlands Organisation for Scientific Research, for the construction and operation of the Virgo detector and the creation and support of the EGO consortium. The authors also gratefully acknowledge research support from these agencies as well as by the Council of Scientific and Industrial Research of India, the Department of Science and Technology, India, the Science & Engineering Research Board (SERB), India, the Ministry of Human Resource Development, India, the Spanish Agencia Estatal de Investigación, the Vicepresidència i Conselleria d’Innovació, Recerca i Turisme and the Conselleria d’Educació i Universitat del Govern de les Illes Balears, the Conselleria d’Educació, Investigació, Cultura i Esport de la Generalitat Valenciana, the National Science Centre of Poland, the Swiss National Science Foundation (SNSF), the Russian Foundation for Basic Research, the Russian Science Foundation, the European Commission, the European Regional Development Funds (ERDF), the Royal Society, the Scottish Funding Council, the Scottish Universities Physics Alliance, the Hungarian Scientific Research Fund (OTKA), the Lyon Institute of Origins (LIO), the Paris Île-de-France Region, the National Research, Development and Innovation Office Hungary (NKFI), the National Research Foundation of Korea, Industry Canada and the Province of Ontario through the Ministry of Economic Development and Innovation, the Natural Science and Engineering Research Council Canada, the Canadian Institute for Advanced Research, the Brazilian Ministry of Science, Technology, Innovations, and Communications, the International Center for Theoretical Physics South American Institute for Fundamental Research (ICTP-SAIFR), the Research Grants Council of Hong Kong, the National Natural Science Foundation of China (NSFC), the Leverhulme Trust, the Research Corporation, the Ministry of Science and Technology (MOST), Taiwan and the Kavli Foundation. The authors gratefully acknowledge the support of the NSF, STFC, MPS, INFN, CNRS and the State of Niedersachsen/Germany for provision of computational resources.

The authors would like to thank N. K. Johnson-McDaniel, W. Kastaun, J. L. Friedman, G. Baym, J. M. Lattimer, L. Rezzolla, M. B. Tsang and M.C. Miller for their useful comments.

-
- [1] J. Aasi *et al.* (LIGO Scientific Collaboration), *Class. Quant. Grav.* **32**, 074001 (2015).
 - [2] F. Acernese *et al.* (The Virgo Collaboration), *Class. Quan-*

- tum Grav. **32**, 024001 (2015), arXiv:1408.3978 [gr-qc].
- [3] B. P. Abbott, R. Abbott, T. D. Abbott, M. R. Abernathy, F. Acernese, K. Ackley, C. Adams, T. Adams, P. Addesso, R. X. Adhikari, and et al., Physical Review Letters **116**, 061102 (2016), arXiv:1602.03837 [gr-qc].
- [4] B. P. Abbott *et al.* (LIGO Scientific Collaboration, Virgo Collaboration, KAGRA Collaboration), Living Rev. Rel. **21**, 3 (2018), arXiv:1304.0670 [gr-qc].
- [5] B. Abbott *et al.* (LIGO Scientific Collaboration, Virgo Collaboration), Phys. Rev. Lett. **119**, 161101 (2017), arXiv:1710.05832 [gr-qc].
- [6] B. P. Abbott *et al.* (Virgo, Fermi-GBM, INTEGRAL, LIGO Scientific Collaboration), Astrophys. J. **848**, L13 (2017), arXiv:1710.05834 [astro-ph.HE].
- [7] A. Goldstein *et al.*, Astrophys. J. **848**, L14 (2017), arXiv:1710.05446 [astro-ph.HE].
- [8] B. P. Abbott *et al.* (GROND, SALT Group, OzGrav, CAASTROs, DFN, DES, INTEGRAL, Virgo, Insight-HXMT, MAXI Team, J-GEM, RATIR, ATLAS, Ice-Cube, LWA, ePESSTO, GRAWITA, RIMAS, SKA South Africa/MeerKAT, H.E.S.S., Fermi Large Area Telescope, IM2H Team, IKI-GW Follow-up, Fermi GBM, Pi of Sky, DWF (Deeper Wider Faster Program), MASTER, AstroSat Cadmium Zinc Telluride Imager Team, Swift, Pierre Auger, ASKAP, VINROUGE, JAGWAR, Chandra Team at McGill University, TTU-NRAO, GROWTH, AGILE Team, MWA, ATCA, AST3, TOROS, Pan-STARRS, NuSTAR, BOOTES, CaltechNRAO, LIGO Scientific Collaboration, High Time Resolution Universe Survey, Nordic Optical Telescope, Las Cumbres Observatory Group, TZAC Consortium, LOFAR, IPN, DLT40, Texas Tech University, HAWC, ANTARES, KU, Dark Energy Camera GW-EM, CALET, Euro VLBI Team, ALMA), Astrophys. J. **848**, L12 (2017), arXiv:1710.05833 [astro-ph.HE].
- [9] D. A. Coulter *et al.*, Science **358**, 1556 (2017), arXiv:1710.05452 [astro-ph.HE].
- [10] E. Troja *et al.*, Nature **551**, 71 (2017), arXiv:1710.05433 [astro-ph.HE].
- [11] D. Haggard, M. Nynka, J. J. Ruan, V. Kalogera, S. Bradley Cenko, P. Evans, and J. A. Kennea, Astrophys. J. **848**, L25 (2017), arXiv:1710.05852 [astro-ph.HE].
- [12] G. Hallinan *et al.*, Science **358**, 1579 (2017), arXiv:1710.05435 [astro-ph.HE].
- [13] A. W. Steiner, S. Gandolfi, F. J. Fattoyev, and W. G. Newton, Phys. Rev. C **91**, 015804 (2015), arXiv:1403.7546 [nucl-th].
- [14] M. B. Tsang, J. R. Stone, F. Camera, P. Danielewicz, S. Gandolfi, K. Hebeler, C. J. Horowitz, J. Lee, W. G. Lynch, Z. Kohley, R. Lemmon, P. Möller, T. Murakami, S. Riordan, X. Roca-Maza, F. Sammarruca, A. W. Steiner, I. Vidaña, and S. J. Yennello, Phys. Rev. C **86**, 015803 (2012), arXiv:1204.0466 [nucl-ex].
- [15] M. Baldo and G. F. Burgio, Progress in Particle and Nuclear Physics **91**, 203 (2016), arXiv:1606.08838 [nucl-th].
- [16] J. M. Lattimer and M. Prakash, Phys. Rep. **621**, 127 (2016), arXiv:1512.07820 [astro-ph.SR].
- [17] M. Oertel, M. Hempel, T. Klähn, and S. Typel, Reviews of Modern Physics **89**, 015007 (2017), arXiv:1610.03361 [astro-ph.HE].
- [18] K. Hebeler, J. M. Lattimer, C. J. Pethick, and A. Schwenk, Astrophys. J. **773**, 11 (2013), arXiv:1303.4662 [astro-ph.SR].
- [19] F. Özel and P. Freire, Ann. Rev. Astron. Astrophys. **54**, 401 (2016), arXiv:1603.02698 [astro-ph.HE].
- [20] A. W. Steiner, C. O. Heinke, S. Bogdanov, C. Li, W. C. G. Ho, A. Bahramian, and S. Han, Mon. Not. Roy. Astron. Soc. **476**, 421 (2018), arXiv:1709.05013 [astro-ph.HE].
- [21] E. E. Flanagan and T. Hinderer, Phys. Rev. D **77**, 021502 (2008).
- [22] J. Vines, E. E. Flanagan, and T. Hinderer, Phys. Rev. D **83**, 084051 (2011), arXiv:1101.1673 [gr-qc].
- [23] T. Damour, A. Nagar, and L. Villain, Phys. Rev. D **85**, 123007 (2012), arXiv:1203.4352 [gr-qc].
- [24] A. Buonanno, B. R. Iyer, E. Ochsner, Y. Pan, and B. S. Sathyaprakash, Phys. Rev. D **80**, 084043 (2009), arXiv:0907.0700 [gr-qc].
- [25] L. Blanchet, Living Rev. Rel. **17**, 2 (2014), arXiv:1310.1528 [gr-qc].
- [26] W. D. Goldberger and I. Z. Rothstein, Phys. Rev. D **73**, 104029 (2006), arXiv:hep-th/0409156 [hep-th].
- [27] W. D. Goldberger, in *Les Houches Summer School - Session 86: Particle Physics and Cosmology: The Fabric of Spacetime Les Houches, France, July 31-August 25, 2006* (2007) arXiv:hep-ph/0701129 [hep-ph].
- [28] T. Damour, B. R. Iyer, and B. S. Sathyaprakash, Phys. Rev. D **63**, 044023 (2001).
- [29] L. Blanchet, T. Damour, B. R. Iyer, C. M. Will, and A. G. Wiseman, Phys. Rev. Lett. **74**, 3515 (1995), arXiv:9501027 [gr-qc].
- [30] L. Blanchet, T. Damour, G. Esposito-Farèse, and B. R. Iyer, Phys. Rev. Lett. **93**, 091101 (2004), arXiv:0406012 [gr-qc].
- [31] T. Damour, P. Jaranowski, and G. Schaefer, Phys. Lett. B **513**, 147 (2001), arXiv:gr-qc/0105038 [gr-qc].
- [32] E. E. Flanagan, Phys. Rev. D **58**, 124030 (1998), arXiv:gr-qc/9706045 [gr-qc].
- [33] T. Damour, in *Les Houches Summer School on Gravitational Radiation Les Houches, France, June 2-21, 1982* (1982).
- [34] S. E. Gralla, Class. Quant. Grav. **35**, 085002 (2018), arXiv:1710.11096 [gr-qc].
- [35] T. Damour, in *Gravitational Radiation*, edited by N. Deruelle and T. Piran (North-Holland, Amsterdam, 1983) pp. 59–144.
- [36] T. Hinderer, Astrophys. J. **677**, 1216 (2008), arXiv:0711.2420 [astro-ph].
- [37] T. Hinderer, B. D. Lackey, R. N. Lang and J. S. Read, Phys. Rev. D **81**, 123016 (2010), arXiv:0911.3535 [astro-ph].
- [38] T. Binnington and E. Poisson, Phys. Rev. D **80**, 084018 (2009), arXiv:0906.1366 [gr-qc].
- [39] T. Damour and A. Nagar, Phys. Rev. D **80**, 084035 (2009), arXiv:0906.0096 [gr-qc].
- [40] E. Poisson, Phys. Rev. D **57**, 5287 (1998), arXiv:gr-qc/9709032 [gr-qc].
- [41] A. Bohé, G. Faye, S. Marsat, and E. K. Porter, Class. Quant. Grav. **32**, 195010 (2015), arXiv:1501.01529 [gr-qc].
- [42] L. Baiotti and L. Rezzolla, Rept. Prog. Phys. **80**, 096901 (2017), arXiv:1607.03540 [gr-qc].
- [43] D. Lai, Monthly Notices of the Royal Astronomical Society **270**, 611 (1994), astro-ph/9404062.
- [44] T. Hinderer, A. Taracchini, F. Foucart, A. Buonanno,

- J. Steinhoff, M. Duez, L. E. Kidder, H. P. Pfeiffer, M. A. Scheel, B. Szilagyi, K. Hotokezaka, K. Kyutoku, M. Shibata, and C. W. Carpenter, *Physical Review Letters* **116**, 181101 (2016), arXiv:1602.00599 [gr-qc].
- [45] N. Andersson and W. C. G. Ho, *Phys. Rev. D* **97**, 023016 (2018), arXiv:1710.05950 [astro-ph.HE].
- [46] W. G. Laarakkers and E. Poisson, *Astrophys. J.* **512**, 282 (1999), arXiv:gr-qc/9709033 [gr-qc].
- [47] G. Pappas and T. A. Apostolatos, (2012), arXiv:1211.6299 [gr-qc].
- [48] M. Agathos, J. Meidam, W. Del Pozzo, T. G. F. Li, M. Tompitak, J. Veitch, S. Vitale, and C. Van Den Broeck, *Phys. Rev. D* **92**, 023012 (2015).
- [49] I. Harry and T. Hinderer, (2018), arXiv:1801.09972 [gr-qc].
- [50] N. V. Krishnendu, K. G. Arun, and C. K. Mishra, *Phys. Rev. Lett.* **119**, 091101 (2017), arXiv:1701.06318 [gr-qc].
- [51] B. P. Abbott *et al.* (LIGO Scientific Collaboration, Virgo Collaboration), *Astrophys. J.* **851**, L16 (2017), arXiv:1710.09320 [astro-ph.HE].
- [52] B. P. Abbott *et al.* (Virgo, LIGO Scientific), (2018), LIGO-P1800061, <https://dcc.ligo.org/LIGO-P1800061/public>, arXiv:1805.11579 [gr-qc].
- [53] S. De, D. Finstad, J. M. Lattimer, D. A. Brown, E. Berger, and C. M. Biwer, *Phys. Rev. Lett.* **121**, 091102 (2018), arXiv:1804.08583 [astro-ph.HE].
- [54] B. Margalit and B. D. Metzger, *The Astrophysical Journal Letters* **850**, L19 (2017).
- [55] A. Bauswein, O. Just, H.-T. Janka, and N. Stergioulas, *The Astrophysical Journal Letters* **850**, L34 (2017).
- [56] E.-P. Zhou, X. Zhou, and A. Li, *Phys. Rev. D* **97**, 083015 (2018), arXiv:1711.04312 [astro-ph.HE].
- [57] L. Rezzolla, E. R. Most, and L. R. Weih, *The Astrophysical Journal Letters* **852**, L25 (2018).
- [58] F. J. Fattoyev, J. Piekarewicz, and C. J. Horowitz, *Phys. Rev. Lett.* **120**, 172702 (2018).
- [59] R. Nandi and P. Char, *Astrophys. J.* **857**, 12 (2018), arXiv:1712.08094 [astro-ph.HE].
- [60] V. Paschalidis, K. Yagi, D. Alvarez-Castillo, D. B. Blaschke, and A. Sedrakian, *Phys. Rev. D* **97**, 084038 (2018), arXiv:1712.00451 [astro-ph.HE].
- [61] M. Ruiz, S. L. Shapiro, and A. Tsokaros, *Phys. Rev. D* **97**, 021501 (2018).
- [62] E. Annala, T. Gorda, A. Kurkela, and A. Vuorinen, *Phys. Rev. Lett.* **120**, 172703 (2018).
- [63] C. Raithel, F. Özel, and D. Psaltis, (2018), arXiv:1803.07687 [astro-ph.HE].
- [64] E. R. Most, L. R. Weih, L. Rezzolla, and J. Schaffner-Bielich, (2018), arXiv:1803.00549 [gr-qc].
- [65] J. Antoniadis, P. C. Freire, N. Wex, T. M. Tauris, R. S. Lynch, *et al.*, *Science* **340**, 1233232 (2013), arXiv:1304.6875 [astro-ph.HE].
- [66] Gravitational Wave Open Science Center (GWOSC), <https://www.gw-openscience.org>.
- [67] C. Pankow *et al.*, (2018), arXiv:1808.03619 [gr-qc].
- [68] J. C. Driggers *et al.* (LIGO Scientific), (2018), arXiv:1806.00532 [astro-ph.IM].
- [69] J. C. Driggers, M. Evans, K. Pepper, and R. Adhikari, *Rev. Sci. Instrum.* **83**, 024501 (2012), arXiv:1112.2224 [gr-qc].
- [70] G. D. Meadors, K. Kawabe, and K. Riles, *Class. Quantum Grav.* **31**, 105014 (2014), arXiv:1311.6835 [astro-ph.IM].
- [71] V. Tiwari *et al.*, *Class. Quantum Grav.* **32**, 165014 (2015), arXiv:1503.07476 [gr-qc].
- [72] J. Veitch, V. Raymond, B. Farr, W. Farr, P. Graff, S. Vitale, B. Aylott, K. Blackburn, N. Christensen, M. Coughlin, W. Del Pozzo, F. Feroz, J. Gair, C.-J. Haster, V. Kalogera, T. Littenberg, I. Mandel, R. O’Shaughnessy, M. Pitkin, C. Rodriguez, C. Röver, T. Sidery, R. Smith, M. Van Der Sluys, A. Vecchio, W. Vousden, and L. Wade, *Phys. Rev. D* **91**, 042003 (2015), arXiv:1409.7215 [gr-qc].
- [73] B. P. Abbott *et al.* (LIGO Scientific Collaboration, Virgo Collaboration), *Phys. Rev. Lett.* **116**, 241102 (2016), arXiv:1602.03840 [gr-qc].
- [74] LIGO Scientific Collaboration and Virgo Collaboration, “LALSuite, https://git.ligo.org/lscsoft/lalsuite/tree/lalinference_o2,” (2017).
- [75] T. B. Littenberg and N. J. Cornish, *Phys. Rev. D* **91**, 084034 (2015), arXiv:1410.3852 [gr-qc].
- [76] N. J. Cornish and T. B. Littenberg, *Class. Quant. Grav.* **32**, 135012 (2015).
- [77] W. M. Farr, B. Farr, and T. Littenberg, *Modelling Calibration Errors In CBC Waveforms*, Tech. Rep. LIGO-T1400682 (LIGO Project, 2015).
- [78] T. M. Tauris *et al.*, *Astrophys. J.* **846**, 170 (2017), arXiv:1706.09438 [astro-ph.HE].
- [79] P. Schmidt, M. Hannam, and S. Husa, *Phys. Rev. D* **86**, 104063 (2012), arXiv:1207.3088 [gr-qc].
- [80] M. Hannam, P. Schmidt, A. Bohé, L. Haegel, S. Husa, F. Ohme, G. Pratten, and M. Pürrer, *Phys. Rev. Lett.* **113**, 151101 (2014), arXiv:1308.3271 [gr-qc].
- [81] P. Schmidt, F. Ohme, and M. Hannam, *Phys. Rev. D* **91**, 024043 (2015), arXiv:1408.1810 [gr-qc].
- [82] S. Husa, S. Khan, M. Hannam, M. Pürrer, F. Ohme, X. J. Forteza, and A. Bohé, *Phys. Rev. D* **93**, 044006 (2016), arXiv:1508.07250 [gr-qc].
- [83] S. Khan, S. Husa, M. Hannam, F. Ohme, M. Pürrer, X. J. Forteza, and A. Bohé, *Phys. Rev. D* **93**, 044007 (2016), arXiv:1508.07253 [gr-qc].
- [84] T. Dietrich, S. Bernuzzi, and W. Tichy, *Phys. Rev. D* **96**, 121501 (2017), arXiv:1706.02969 [gr-qc].
- [85] A. Bohé *et al.*, *Phys. Rev. D* **95**, 044028 (2017), arXiv:1611.03703 [gr-qc].
- [86] S. Bernuzzi, A. Nagar, T. Dietrich, and T. Damour, *Phys. Rev. Lett.* **114**, 161103 (2015), arXiv:1412.4553 [gr-qc].
- [87] B. D. Lackey, S. Bernuzzi, C. R. Galley, J. Meidam, and C. Van Den Broeck, *Phys. Rev. D* **95**, 104036 (2017), arXiv:1610.04742 [gr-qc].
- [88] T. Hinderer *et al.*, *Phys. Rev. Lett.* **116**, 181101 (2016), arXiv:1602.00599 [gr-qc].
- [89] J. Steinhoff, T. Hinderer, A. Buonanno, and A. Taracchini, *Phys. Rev. D* **94**, 104028 (2016), arXiv:1608.01907 [gr-qc].
- [90] B. S. Sathyaprakash and S. V. Dhurandhar, *Phys. Rev. D* **44**, 3819 (1991).
- [91] A. Bohé, S. Marsat, and L. Blanchet, *Class. Quant. Grav.* **30**, 135009 (2013), arXiv:1303.7412 [gr-qc].
- [92] K. Arun, A. Buonanno, G. Faye, and E. Ochsner, *Phys. Rev. D* **79**, 104023 (2009), arXiv:0810.5336 [gr-qc].
- [93] B. Mikoczi, M. Vasuth, and L. A. Gergely, *Phys. Rev. D*

- 71, 124043 (2005), arXiv:astro-ph/0504538 [astro-ph].
- [94] C. K. Mishra, A. Kela, K. G. Arun, and G. Faye, Phys. Rev. D **93**, 084054 (2016), arXiv:1601.05588 [gr-qc].
- [95] A. Taracchini, A. Buonanno, Y. Pan, T. Hinderer, M. Boyle, D. A. Hemberger, L. E. Kidder, G. Lovelace, A. H. Mroué, H. P. Pfeiffer, M. A. Scheel, B. Szilágyi, N. W. Taylor, and A. Zenginoglu, Phys. Rev. D **89**, 061502 (2014), arXiv:1311.2544 [gr-qc].
- [96] E. Barausse and A. Buonanno, Phys. Rev. D **81**, 084024 (2010), arXiv:0912.3517 [gr-qc].
- [97] A. Buonanno and T. Damour, Phys. Rev. D **62**, 064015 (2000), arXiv:gr-qc/0001013 [gr-qc].
- [98] A. Buonanno and T. Damour, Phys. Rev. D **59**, 084006 (1999), arXiv:gr-qc/9811091 [gr-qc].
- [99] L. Wade, J. D. E. Creighton, E. Ochsner, B. D. Lackey, B. F. Farr, T. B. Littenberg, and V. Raymond, Phys. Rev. D **89**, 103012 (2014), arXiv:1402.5156 [gr-qc].
- [100] T. Dietrich *et al.*, (2018), arXiv:1804.02235 [gr-qc].
- [101] K. Yagi and N. Yunes, Science **341**, 365 (2013), arXiv:1302.4499 [gr-qc].
- [102] K. Yagi and N. Yunes, Phys. Rev. D **88**, 023009 (2013), arXiv:1303.1528 [gr-qc].
- [103] K. Chatziioannou, K. Yagi, A. Klein, N. Cornish, and N. Yunes, Phys. Rev. D **92**, 104008 (2015), arXiv:1508.02062 [gr-qc].
- [104] K. Yagi and N. Yunes, Phys. Rept. **681**, 1 (2017), arXiv:1608.02582 [gr-qc].
- [105] K. Yagi and N. Yunes, Class. Quant. Grav. **33**, 13LT01 (2016), arXiv:1512.02639 [gr-qc].
- [106] K. Chatziioannou, C.-J. Haster, and A. Zimmerman, Phys. Rev. D **97**, 104036 (2018), arXiv:1804.03221 [gr-qc].
- [107] A. Maselli, V. Cardoso, V. Ferrari, L. Gualtieri, and P. Pani, Phys. Rev. D **88**, 023007 (2013), arXiv:1304.2052 [gr-qc].
- [108] M. Urbanec, J. C. Miller, and Z. Stuchlik, Mon. Not. Roy. Astron. Soc. **433**, 1903 (2013), arXiv:1301.5925 [astro-ph.SR].
- [109] L. Lindblom, (2018), arXiv:1804.04072 [astro-ph.HE].
- [110] L. Lindblom, Phys. Rev. D **82**, 103011 (2010).
- [111] L. Lindblom and N. M. Indik, Phys. Rev. D **86**, 084003 (2012), arXiv:1207.3744 [astro-ph.HE].
- [112] L. Lindblom and N. M. Indik, Phys. Rev. D **89**, 064003 (2014), [Erratum: Phys. Rev.D93,no.12,129903(2016)], arXiv:1310.0803 [astro-ph.HE].
- [113] F. Douchin and P. Haensel, Astron. Astrophys **380**, 151 (2001), arXiv:astro-ph/0111092.
- [114] J. M. Lattimer and M. Prakash, Astrophys. J. **550**, 426 (2001), arXiv:astro-ph/0002232 [astro-ph].
- [115] J. S. Read, B. D. Lackey, B. J. Owen, and J. L. Friedman, Phys. Rev. D **79**, 124032 (2009), arXiv:0812.2163 [astro-ph].
- [116] G. Raaijmakers, T. E. Riley, and A. L. Watts, (2018), arXiv:1804.09087 [astro-ph.HE].
- [117] M. F. Carney, L. E. Wade, and B. S. Irwin, Phys. Rev. D **98**, 063004 (2018).
- [118] B. D. Lackey and L. Wade, Phys. Rev. D **91**, 043002 (2015), arXiv:1410.8866 [gr-qc].
- [119] S. L. Shapiro and S. A. Teukolsky, *Black holes, white dwarfs, and neutron stars: Their physics of compact objects. New York, Wiley-Interscience, 1983, 663 p.* (1983).
- [120] W. Del Pozzo, T. G. F. Li, M. Agathos, C. Van Den Broeck, and S. Vitale, Phys. Rev. Lett. **111**, 071101 (2013).
- [121] R. B. Wiringa, V. Fiks, and A. Fabrocini, Phys. Rev. C **38**, 1010 (1988).
- [122] A. Akmal, V. R. Pandharipande, and D. G. Ravenhall, Phys. Rev. C **58**, 1804 (1998), arXiv:nucl-th/9804027.
- [123] H. Mütter, M. Prakash, and T. L. Ainsworth, Phys. Lett. B **199**, 469 (1987).
- [124] B. D. Lackey, M. Nayyar, and B. J. Owen, Phys. Rev. D **73**, 024021 (2006), arXiv:astro-ph/0507312.
- [125] H. Müller and B. D. Serot, Nucl. Phys. **A606**, 508 (1996), arXiv:nucl-th/9603037 [nucl-th].
- [126] A. W. Steiner, J. M. Lattimer, and E. F. Brown, Astrophys. J. **722**, 33 (2010), arXiv:1005.0811 [astro-ph.HE].
- [127] J. Nattila, M. C. Miller, A. W. Steiner, J. J. E. Kajava, V. F. Suleimanov, and J. Poutanen, Astron. Astrophys. **608**, A31 (2017), arXiv:1709.09120 [astro-ph.HE].
- [128] M. Shibata, S. Fujibayashi, K. Hotokezaka, K. Kiuchi, K. Kyutoku, Y. Sekiguchi, and M. Tanaka, Phys. Rev. **D96**, 123012 (2017), arXiv:1710.07579 [astro-ph.HE].
- [129] D. Radice, A. Perego, F. Zappa, and S. Bernuzzi, Astrophys. J. **852**, L29 (2018), arXiv:1711.03647 [astro-ph.HE].
- [130] M. W. Coughlin *et al.*, (2018), arXiv:1805.09371 [astro-ph.HE].
- [131] Gravitational Wave Open Science Center (GWOSC), <https://doi.org/10.7935/K5B8566F> (2017).

Authors

B. P. Abbott,¹ R. Abbott,¹ T. D. Abbott,² F. Acernese,^{3,4} K. Ackley,⁵ C. Adams,⁶ T. Adams,⁷ P. Addesso,⁸ R. X. Adhikari,¹ V. B. Adya,^{9,10} C. Affeldt,^{9,10} B. Agarwal,¹¹ M. Agathos,¹² K. Agatsuma,¹³ N. Aggarwal,¹⁴ O. D. Aguiar,¹⁵ L. Aiello,^{16,17} A. Ain,¹⁸ P. Ajith,¹⁹ B. Allen,^{9,20,10} G. Allen,¹¹ A. Allocca,^{21,22} M. A. Aloy,²³ P. A. Altin,²⁴ A. Amato,²⁵ A. Ananyeva,¹ S. B. Anderson,¹ W. G. Anderson,²⁰ S. V. Angelova,²⁶ S. Antier,²⁷ S. Appert,¹ K. Arai,¹ M. C. Araya,¹ J. S. Areeda,²⁸ M. Arène,²⁹ N. Arnaud,^{27,30} K. G. Arun,³¹ S. Ascenzi,^{32,33} G. Ashton,⁵ M. Ast,³⁴ S. M. Aston,⁶ P. Astone,³⁵ D. V. Atallah,³⁶ F. Aubin,⁷ P. Aufmuth,¹⁰ C. Aubert,⁹ K. AultONEal,³⁷ C. Austin,² A. Avila-Alvarez,²⁸ S. Babak,^{38,29} P. Bacon,²⁹ F. Badaracco,^{16,17} M. K. M. Bader,¹³ S. Bae,³⁹ P. T. Baker,⁴⁰ F. Baldaccini,^{41,42} G. Ballardini,³⁰ S. W. Ballmer,⁴³ S. Banagiri,⁴⁴ J. C. Barayoga,¹ S. E. Barclay,⁴⁵ B. C. Barish,¹ D. Barker,⁴⁶ K. Barkett,⁴⁷ S. Barnum,¹⁴ F. Barone,^{3,4} B. Barr,⁴⁵ L. Barsotti,¹⁴ M. Barsuglia,²⁹ D. Barta,⁴⁸ J. Bartlett,⁴⁶ I. Bartos,⁴⁹ R. Bassiri,⁵⁰ A. Basti,^{21,22} J. C. Batch,⁴⁶ M. Bawaj,^{51,42} J. C. Bayley,⁴⁵ M. Bazzan,^{52,53} B. Bécsy,⁵⁴ C. Beer,⁹ M. Bejger,⁵⁵ I. Belahcene,²⁷ A. S. Bell,⁴⁵ D. Beniwal,⁵⁶ M. Bensch,^{9,10} B. K. Berger,¹ G. Bergmann,^{9,10} S. Bernuzzi,^{57,58} J. J. Bero,⁵⁹ C. P. L. Berry,⁶⁰ D. Bersanetti,⁶¹ A. Bertolini,¹³ J. Betzwieser,⁶ R. Bhandare,⁶² I. A. Bilenko,⁶³ S. A. Bilgili,⁴⁰ G. Billingsley,¹ C. R. Billman,⁴⁹ J. Birch,⁶ R. Birney,²⁶ O. Birnholtz,⁵⁹ S. Biscans,^{1,14} S. Biscoveanu,⁵ A. Bisht,^{9,10} M. Bitossi,^{30,22} M. A. Bizouard,²⁷ J. K. Blackburn,¹ J. Blackman,⁴⁷ C. D. Blair,⁶ D. G. Blair,⁶⁴ R. M. Blair,⁴⁶ S. Bloemen,⁶⁵ O. Bock,⁹ N. Bode,^{9,10} M. Boer,⁶⁶ Y. Boetzel,⁶⁷ G. Bogaert,⁶⁶ A. Bohe,³⁸ F. Bondu,⁶⁸ E. Bonilla,⁵⁰ R. Bonnand,⁷ P. Booker,^{9,10} B. A. Boom,¹³ C. D. Booth,³⁶ R. Bork,¹ V. Boschi,³⁰ S. Bose,^{69,18} K. Bossie,⁶ V. Bossilkov,⁶⁴ J. Bosveld,⁶⁴ Y. Bouffanais,²⁹ A. Bozzi,³⁰ C. Bradaschia,²² P. R. Brady,²⁰ A. Bramley,⁶ M. Branchesi,^{16,17} J. E. Brau,⁷⁰ T. Briant,⁷¹ F. Brighenti,^{72,73} A. Brillet,⁶⁶ M. Brinkmann,^{9,10} V. Brisson,^{27,*} P. Brockill,²⁰ A. F. Brooks,¹ D. D. Brown,⁵⁶ S. Brunett,¹ C. C. Buchanan,² A. Buikema,¹⁴ T. Bulik,⁷⁴ H. J. Bulten,^{75,13} A. Buonanno,^{38,76} D. Buskulic,⁷ C. Buy,²⁹ R. L. Byer,⁵⁰ M. Cabero,⁹ L. Cadonati,⁷⁷ G. Cagnoli,^{25,78} C. Cahillane,¹ J. Calderón Bustillo,⁷⁷ T. A. Callister,¹ E. Calloni,^{79,4} J. B. Camp,⁸⁰ M. Canepa,^{81,61} P. Canizares,⁶⁵ K. C. Cannon,⁸² H. Cao,⁵⁶ J. Cao,⁸³ C. D. Capano,⁹ E. Capocasa,²⁹ F. Carbognani,³⁰ S. Caride,⁸⁴ M. F. Carney,⁸⁵ G. Carullo,²¹ J. Casanueva Diaz,²² C. Casentini,^{32,33} S. Caudill,^{13,20} M. Cavaglià,⁸⁶ F. Cavalier,²⁷ R. Cavalieri,³⁰ G. Cella,²² C. B. Cepeda,¹ P. Cerdá-Durán,²³ G. Cerretani,^{21,22} E. Cesarini,^{87,33} O. Chaibi,⁶⁶ S. J. Chamberlin,⁸⁸ M. Chan,⁴⁵ S. Chao,⁸⁹ P. Charlton,⁹⁰ E. Chase,⁹¹ E. Chassande-Mottin,²⁹ D. Chatterjee,²⁰ K. Chatzioannou,⁹² B. D. Cheeseboro,⁴⁰ H. Y. Chen,⁹³ X. Chen,⁶⁴ Y. Chen,⁴⁷ H.-P. Cheng,⁴⁹ H. Y. Chia,⁴⁹ A. Chincarini,⁶¹ A. Chiummo,³⁰ T. Chmiel,⁸⁵ H. S. Cho,⁹⁴ M. Cho,⁷⁶ J. H. Chow,²⁴ N. Christensen,^{95,66} Q. Chu,⁶⁴ A. J. K. Chua,⁴⁷ S. Chua,⁷¹ K. W. Chung,⁹⁶ S. Chung,⁶⁴ G. Ciani,^{52,53,49} A. A. Ciobanu,⁵⁶ R. Ciolfi,^{97,98} F. Cipriano,⁶⁶ C. E. Cirelli,⁵⁰ A. Cirone,^{81,61} F. Clara,⁴⁶ J. A. Clark,⁷⁷ P. Clearwater,⁹⁹ F. Cleva,⁶⁶ C. Cocchieri,⁸⁶ E. Coccia,^{16,17} P.-F. Cohadon,⁷¹ D. Cohen,²⁷ A. Colla,^{100,35} C. G. Collette,¹⁰¹ C. Collins,⁶⁰ L. R. Cominsky,¹⁰² M. Constancio Jr.,¹⁵ L. Conti,⁵³ S. J. Cooper,⁶⁰ P. Corban,⁶ T. R. Corbitt,² I. Cordero-Carrión,¹⁰³ K. R. Corley,¹⁰⁴ N. Cornish,¹⁰⁵ A. Corsi,⁸⁴ S. Cortese,³⁰ C. A. Costa,¹⁵ R. Cotesta,³⁸ M. W. Coughlin,¹ S. B. Coughlin,^{36,91} J.-P. Coulon,⁶⁶ S. T. Countryman,¹⁰⁴ P. Couvares,¹ P. B. Covas,¹⁰⁶ E. E. Cowan,⁷⁷ D. M. Coward,⁶⁴ M. J. Cowart,⁶ D. C. Coyne,¹ R. Coyne,¹⁰⁷ J. D. E. Creighton,²⁰ T. D. Creighton,¹⁰⁸ J. Cripe,² S. G. Crowder,¹⁰⁹ T. J. Cullen,² A. Cumming,⁴⁵ L. Cunningham,⁴⁵ E. Cuoco,³⁰ T. Dal Canton,⁸⁰ G. Dálya,⁵⁴ S. L. Danilishin,^{10,9} S. D'Antonio,³³ K. Danzmann,^{9,10} A. Dasgupta,¹¹⁰ C. F. Da Silva Costa,⁴⁹ V. Dattilo,³⁰ I. Dave,⁶² M. Davier,²⁷ D. Davis,⁴³ E. J. Daw,¹¹¹ B. Day,⁷⁷ D. DeBra,⁵⁰ M. Deenadayalan,¹⁸ J. Degallaix,²⁵ M. De Laurentis,^{79,4} S. Deléglise,⁷¹ W. Del Pozzo,^{21,22} N. Demos,¹⁴ T. Denker,^{9,10} T. Dent,⁹ R. De Pietri,^{57,58} J. Derby,²⁸ V. Dergachev,⁹ R. De Rosa,^{79,4} C. De Rossi,^{25,30} R. DeSalvo,¹¹² O. de Varona,^{9,10} S. Dhurandhar,¹⁸ M. C. Díaz,¹⁰⁸ T. Dietrich,^{13,38} L. Di Fiore,⁴ M. Di Giovanni,^{113,98} T. Di Girolamo,^{79,4} A. Di Lieto,^{21,22} B. Ding,¹⁰¹ S. Di Pace,^{100,35} I. Di Palma,^{100,35} F. Di Renzo,^{21,22} A. Dmitriev,⁶⁰ Z. Doctor,⁹³ V. Dolique,²⁵ F. Donovan,¹⁴ K. L. Dooley,^{36,86} S. Doravari,^{9,10} I. Dorrington,³⁶ M. Dovale Álvarez,⁶⁰ T. P. Downes,²⁰ M. Drago,^{9,16,17} C. Dreissigacker,^{9,10} J. C. Driggers,⁴⁶ Z. Du,⁸³ P. Dupej,⁴⁵ S. E. Dwyer,⁴⁶ P. J. Easter,⁵ T. B. Edo,¹¹¹ M. C. Edwards,⁹⁵ A. Effler,⁶ H.-B. Eggenstein,^{9,10} P. Ehrens,¹ J. Eichholz,¹ S. S. Eikenberry,⁴⁹ M. Eisenmann,⁷ R. A. Eisenstein,¹⁴ R. C. Essick,⁹³ H. Estelles,¹⁰⁶ D. Estevez,⁷ Z. B. Etienne,⁴⁰ T. Etzel,¹ M. Evans,¹⁴ T. M. Evans,⁶ V. Fafone,^{32,33,16} H. Fair,⁴³ S. Fairhurst,³⁶ X. Fan,⁸³ S. Farinon,⁶¹ B. Farr,⁷⁰ W. M. Farr,⁶⁰ E. J. Fauchon-Jones,³⁶ M. Favata,¹¹⁴ M. Fays,³⁶ C. Fee,⁸⁵ H. Fehrmann,⁹ J. Feicht,¹ M. M. Fejer,⁵⁰ F. Feng,²⁹ A. Fernandez-Galiana,¹⁴ I. Ferrante,^{21,22} E. C. Ferreira,¹⁵ F. Ferrini,³⁰ F. Fidecaro,^{21,22} I. Fiori,³⁰ D. Fiorucci,²⁹ M. Fishbach,⁹³ R. P. Fisher,⁴³ J. M. Fishner,¹⁴ M. Fitz-Axen,⁴⁴ R. Flamini,^{7,115} M. Fletcher,⁴⁵ H. Fong,⁹² J. A. Font,^{23,116} P. W. F. Forsyth,²⁴ S. S. Forsyth,⁷⁷ J.-D. Fournier,⁶⁶ S. Frasca,^{100,35} F. Frasconi,²² Z. Frei,⁵⁴ A. Freise,⁶⁰ R. Frey,⁷⁰ V. Frey,²⁷ P. Fritschel,¹⁴ V. V. Frolov,⁶ P. Fulda,⁴⁹ M. Fyffe,⁶ H. A. Gabbard,⁴⁵ B. U. Gadre,¹⁸ S. M. Gaebel,⁶⁰ J. R. Gair,¹¹⁷ L. Gammaitoni,⁴¹ M. R. Ganija,⁵⁶ S. G. Gaonkar,¹⁸ A. Garcia,²⁸

- C. García-Quirós,¹⁰⁶ F. Garufi,^{79,4} B. Gateley,⁴⁶ S. Gaudio,³⁷ G. Gaur,¹¹⁸ V. Gayathri,¹¹⁹ G. Gemme,⁶¹ E. Genin,³⁰
A. Gennai,²² D. George,¹¹ J. George,⁶² L. Gergely,¹²⁰ V. Germain,⁷ S. Ghonge,⁷⁷ Abhirup Ghosh,¹⁹ Archisman Ghosh,¹³
S. Ghosh,²⁰ B. Giacomazzo,^{113,98} J. A. Giaime,^{2,6} K. D. Giardino,⁶ A. Giazotto,^{22,†} K. Gill,³⁷ G. Giordano,^{3,4}
L. Glover,¹¹² E. Goetz,⁴⁶ R. Goetz,⁴⁹ B. Goncharov,⁵ G. González,² J. M. Gonzalez Castro,^{21,22} A. Gopakumar,¹²¹
M. L. Gorodetsky,⁶³ S. E. Gossan,¹ M. Gosselin,³⁰ R. Gouaty,⁷ A. Grado,^{122,4} C. Graef,⁴⁵ M. Granata,²⁵ A. Grant,⁴⁵
S. Gras,¹⁴ C. Gray,⁴⁶ G. Greco,^{72,73} A. C. Green,⁶⁰ R. Green,³⁶ E. M. Gretarsson,³⁷ P. Groot,⁶⁵ H. Grote,³⁶
S. Grunewald,³⁸ P. Gruning,²⁷ G. M. Guidi,^{72,73} H. K. Gulati,¹¹⁰ X. Guo,⁸³ A. Gupta,⁸⁸ M. K. Gupta,¹¹⁰ K. E. Gushwa,¹
E. K. Gustafson,¹ R. Gustafson,¹²³ O. Halim,^{17,16} B. R. Hall,⁶⁹ E. D. Hall,¹⁴ E. Z. Hamilton,³⁶ H. F. Hamilton,¹²⁴
G. Hammond,⁴⁵ M. Haney,⁶⁷ M. M. Hanke,^{9,10} J. Hanks,⁴⁶ C. Hanna,⁸⁸ M. D. Hannam,³⁶ O. A. Hannuksela,⁹⁶
J. Hanson,⁶ T. Hardwick,² J. Harms,^{16,17} G. M. Harry,¹²⁵ I. W. Harry,³⁸ M. J. Hart,⁴⁵ C.-J. Haster,⁹² K. Haughian,⁴⁵
J. Healy,⁵⁹ A. Heidmann,⁷¹ M. C. Heintze,⁶ H. Heitmann,⁶⁶ P. Hello,²⁷ G. Hemming,³⁰ M. Hendry,⁴⁵ I. S. Heng,⁴⁵
J. Hennig,⁴⁵ A. W. Heptonstall,¹ F. J. Hernandez,⁵ M. Heurs,^{9,10} S. Hild,⁴⁵ T. Hinderer,⁶⁵ W. C. G. Ho,¹²⁶ D. Hoak,³⁰
S. Hochheim,^{9,10} D. Hofman,²⁵ N. A. Holland,²⁴ K. Holt,⁶ D. E. Holz,⁹³ P. Hopkins,³⁶ C. Horst,²⁰ J. Hough,⁴⁵
E. A. Houston,⁴⁵ E. J. Howell,⁶⁴ A. Hreibi,⁶⁶ E. A. Huerta,¹¹ D. Huet,²⁷ B. Hughey,³⁷ M. Hulko,¹ S. Husa,¹⁰⁶
S. H. Huttner,⁴⁵ T. Huynh-Dinh,⁶ A. Iess,^{32,33} N. Indik,⁹ C. Ingram,⁵⁶ R. Inta,⁸⁴ G. Intini,^{100,35} B. S. Irwin,⁸⁵ H. N. Isa,⁴⁵
J.-M. Isac,⁷¹ M. Isi,¹ B. R. Iyer,¹⁹ K. Izumi,⁴⁶ T. Jacqmin,⁷¹ K. Jani,⁷⁷ P. Jaranowski,¹²⁷ D. S. Johnson,¹¹ W. W. Johnson,²
D. I. Jones,¹²⁶ R. Jones,⁴⁵ R. J. G. Jonker,¹³ L. Ju,⁶⁴ J. Junker,^{9,10} C. V. Kalaghatgi,³⁶ V. Kalogera,⁹¹ B. Kamai,¹
S. Kandhasamy,⁶ G. Kang,³⁹ J. B. Kanner,¹ S. J. Kapadia,²⁰ S. Karki,⁷⁰ K. S. Karvinen,^{9,10} M. Kasprzack,² M. Katolik,¹¹
S. Katsanevas,³⁰ E. Katsavounidis,¹⁴ W. Katzman,⁶ S. Kaufer,^{9,10} K. Kawabe,⁴⁶ N. V. Keerthana,¹⁸ F. Kéfélian,⁶⁶
D. Keitel,⁴⁵ A. J. Kemball,¹¹ R. Kennedy,¹¹¹ J. S. Key,¹²⁸ F. Y. Khalili,⁶³ B. Khamesra,⁷⁷ H. Khan,²⁸ I. Khan,^{16,33}
S. Khan,⁹ Z. Khan,¹¹⁰ E. A. Khazanov,¹²⁹ N. Kijbunchoo,²⁴ Chunglee Kim,¹³⁰ J. C. Kim,¹³¹ K. Kim,⁹⁶ W. Kim,⁵⁶
W. S. Kim,¹³² Y.-M. Kim,¹³³ E. J. King,⁵⁶ P. J. King,⁴⁶ M. Kinley-Hanlon,¹²⁵ R. Kirchhoff,^{9,10} J. S. Kissel,⁴⁶
L. Kleybolte,³⁴ S. Klimenko,⁴⁹ T. D. Knowles,⁴⁰ P. Koch,^{9,10} S. M. Koehlenbeck,^{9,10} S. Koley,¹³ V. Kondrashov,¹
A. Kontos,¹⁴ M. Korobko,³⁴ W. Z. Korth,¹ I. Kowalska,⁷⁴ D. B. Kozak,¹ C. Krämer,⁹ V. Kringel,^{9,10} B. Krishnan,⁹
A. Królak,^{134,135} G. Kuehn,^{9,10} P. Kumar,¹³⁶ R. Kumar,¹¹⁰ S. Kumar,¹⁹ L. Kuo,⁸⁹ A. Kutynia,¹³⁴ S. Kwang,²⁰
B. D. Lackey,³⁸ K. H. Lai,⁹⁶ M. Landry,⁴⁶ P. Landry,⁹³ R. N. Lang,¹³⁷ J. Lange,⁵⁹ B. Lantz,⁵⁰ R. K. Lanza,¹⁴
A. Lartaux-Vollard,²⁷ P. D. Lasky,⁵ M. Laxen,⁶ A. Lazzarini,¹ C. Lazzaro,⁵³ P. Leaci,^{100,35} S. Leavey,^{9,10} C. H. Lee,⁹⁴
H. K. Lee,¹³⁸ H. M. Lee,¹³⁰ H. W. Lee,¹³¹ K. Lee,⁴⁵ J. Lehmann,^{9,10} A. Lenon,⁴⁰ M. Leonardi,^{9,10,115} N. Leroy,²⁷
N. Letendre,⁷ Y. Levin,⁵ J. Li,⁸³ T. G. F. Li,⁹⁶ X. Li,⁴⁷ S. D. Linker,¹¹² T. B. Littenberg,¹³⁹ J. Liu,⁶⁴ X. Liu,²⁰
R. K. L. Lo,⁹⁶ N. A. Lockerbie,²⁶ L. T. London,³⁶ A. Longo,^{140,141} M. Lorenzini,^{16,17} V. Lorette,¹⁴² M. Lormand,⁶
G. Losurdo,²² J. D. Lough,^{9,10} C. O. Lousto,⁵⁹ G. Lovelace,²⁸ H. Lück,^{9,10} D. Lumaca,^{32,33} A. P. Lundgren,⁹ R. Lynch,¹⁴
Y. Ma,⁴⁷ R. Macas,³⁶ S. Macfoy,²⁶ B. Machenschalk,⁹ M. MacInnis,¹⁴ D. M. Macleod,³⁶ I. Magaña Hernandez,²⁰
F. Magaña-Sandoval,⁴³ L. Magaña Zertuche,⁸⁶ R. M. Magee,⁸⁸ E. Majorana,³⁵ I. Maksimovic,¹⁴² N. Man,⁶⁶ V. Mandic,⁴⁴
V. Mangano,⁴⁵ G. L. Mansell,²⁴ M. Manske,^{20,24} M. Mantovani,³⁰ F. Marchesoni,^{51,42} F. Marion,⁷ S. Márka,¹⁰⁴
Z. Márka,¹⁰⁴ C. Markakis,¹¹ A. S. Markosyan,⁵⁰ A. Markowitz,¹ E. Maros,¹ A. Marquina,¹⁰³ F. Martelli,^{72,73}
L. Martellini,⁶⁶ I. W. Martin,⁴⁵ R. M. Martin,¹¹⁴ D. V. Martynov,¹⁴ K. Mason,¹⁴ E. Massera,¹¹¹ A. Masserot,⁷
T. J. Massinger,¹ M. Masso-Reid,⁴⁵ S. Mastrogiovanni,^{100,35} A. Matas,⁴⁴ F. Matichard,^{1,14} L. Matone,¹⁰⁴ N. Mavalvala,¹⁴
N. Mazumder,⁶⁹ J. J. McCann,⁶⁴ R. McCarthy,⁴⁶ D. E. McClelland,²⁴ S. McCormick,⁶ L. McCuller,¹⁴ S. C. McGuire,¹⁴³
J. McIver,¹ D. J. McManus,²⁴ T. McRae,²⁴ S. T. McWilliams,⁴⁰ D. Meacher,⁸⁸ G. D. Meadors,⁵ M. Mehmet,^{9,10}
J. Meidam,¹³ E. Mejuto-Villa,⁸ A. Melatos,⁹⁹ G. Mendell,⁴⁶ D. Mendoza-Gandara,^{9,10} R. A. Mercer,²⁰ L. Mereni,²⁵
E. L. Merilh,⁴⁶ M. Merzougui,⁶⁶ S. Meshkov,¹ C. Messenger,⁴⁵ C. Messick,⁸⁸ R. Metzdrorf,⁷¹ P. M. Meyers,⁴⁴
H. Miao,⁶⁰ C. Michel,²⁵ H. Middleton,⁹⁹ E. E. Mikhailov,¹⁴⁴ L. Milano,^{79,4} A. L. Miller,⁴⁹ A. Miller,^{100,35} B. B. Miller,⁹¹
J. Miller,¹⁴ M. Millhouse,¹⁰⁵ J. Mills,³⁶ M. C. Milovich-Goff,¹¹² O. Minazzoli,^{66,145} Y. Minenkov,³³ J. Ming,^{9,10}
C. Mishra,¹⁴⁶ S. Mitra,¹⁸ V. P. Mitrofanov,⁶³ G. Mitselmakher,⁴⁹ R. Mittleman,¹⁴ D. Moffa,⁸⁵ K. Mogushi,⁸⁶
M. Mohan,³⁰ S. R. P. Mohapatra,¹⁴ M. Montani,^{72,73} C. J. Moore,¹² D. Moraru,⁴⁶ G. Moreno,⁴⁶ S. Morisaki,⁸²
B. Mours,⁷ C. M. Mow-Lowry,⁶⁰ G. Mueller,⁴⁹ A. W. Muir,³⁶ Arunava Mukherjee,^{9,10} D. Mukherjee,²⁰ S. Mukherjee,¹⁰⁸
N. Mukund,¹⁸ A. Mullavey,⁶ J. Munch,⁵⁶ E. A. Muñoz,⁴³ M. Muratore,³⁷ P. G. Murray,⁴⁵ A. Nagar,^{87,147,148}
K. Napier,⁷⁷ I. Nardecchia,^{32,33} L. Naticchioni,^{100,35} R. K. Nayak,¹⁴⁹ J. Neilson,¹¹² G. Nelemans,^{65,13} T. J. N. Nelson,⁶
M. Nery,^{9,10} A. Neunzert,¹²³ L. Nevin,¹ J. M. Newport,¹²⁵ K. Y. Ng,¹⁴ S. Ng,⁵⁶ P. Nguyen,⁷⁰ T. T. Nguyen,²⁴
D. Nichols,⁶⁵ A. B. Nielsen,⁹ S. Nissanke,^{65,13} A. Nitz,⁹ F. Nocera,³⁰ D. Nolting,⁶ C. North,³⁶ L. K. Nuttall,³⁶
M. Obergaulinger,²³ J. Oberling,⁴⁶ B. D. O'Brien,⁴⁹ G. D. O'Dea,¹¹² G. H. Ogin,¹⁵⁰ J. J. Oh,¹³² S. H. Oh,¹³²

F. Ohme,⁹ H. Ohta,⁸² M. A. Okada,¹⁵ M. Oliver,¹⁰⁶ P. Oppermann,^{9,10} Richard J. Oram,⁶ B. O'Reilly,⁶ R. Ormiston,⁴⁴ L. F. Ortega,⁴⁹ R. O'Shaughnessy,⁵⁹ S. Ossokine,³⁸ D. J. Ottaway,⁵⁶ H. Overmier,⁶ B. J. Owen,⁸⁴ A. E. Pace,⁸⁸ G. Pagano,^{21,22} J. Page,¹³⁹ M. A. Page,⁶⁴ A. Pai,¹¹⁹ S. A. Pai,⁶² J. R. Palamos,⁷⁰ O. Palashov,¹²⁹ C. Palomba,³⁵ A. Pal-Singh,³⁴ Howard Pan,⁸⁹ Huang-Wei Pan,⁸⁹ B. Pang,⁴⁷ P. T. H. Pang,⁹⁶ C. Pankow,⁹¹ F. Pannarale,³⁶ B. C. Pant,⁶² F. Paoletti,²² A. Paoli,³⁰ M. A. Papa,^{9,20,10} A. Parida,¹⁸ W. Parker,⁶ D. Pascucci,⁴⁵ A. Pasqualetti,³⁰ R. Passaquietti,^{21,22} D. Passuello,²² M. Patil,¹³⁵ B. Patricelli,^{151,22} B. L. Pearlstone,⁴⁵ C. Pedersen,³⁶ M. Pedraza,¹ R. Pedurand,^{25,152} L. Pekowsky,⁴³ A. Pele,⁶ S. Penn,¹⁵³ A. Perego,^{154,58} C. J. Perez,⁴⁶ A. Perreca,^{113,98} L. M. Perri,⁹¹ H. P. Pfeiffer,^{92,38} M. Phelps,⁴⁵ K. S. Phukon,¹⁸ O. J. Piccinni,^{100,35} M. Pichot,⁶⁶ F. Piergiovanni,^{72,73} V. Pierro,⁸ G. Pillant,³⁰ L. Pinard,²⁵ I. M. Pinto,⁸ M. Pirello,⁴⁶ M. Pitkin,⁴⁵ R. Poggiani,^{21,22} P. Popolizio,³⁰ E. K. Porter,²⁹ L. Possenti,^{155,73} A. Post,⁹ J. Powell,¹⁵⁶ J. Prasad,¹⁸ J. W. W. Pratt,³⁷ G. Pratten,¹⁰⁶ V. Predoi,³⁶ T. Prestegard,²⁰ M. Principe,⁸ S. Privitera,³⁸ G. A. Prodi,^{113,98} L. G. Prokhorov,⁶³ O. Puncken,^{9,10} M. Punturo,⁴² P. Puppò,³⁵ M. Pürner,³⁸ H. Qi,²⁰ V. Quetschke,¹⁰⁸ E. A. Quintero,¹ R. Quitzow-James,⁷⁰ F. J. Raab,⁴⁶ D. S. Rabeling,²⁴ H. Radkins,⁴⁶ P. Raffai,⁵⁴ S. Raja,⁶² C. Rajan,⁶² B. Rajbhandari,⁸⁴ M. Rakhmanov,¹⁰⁸ K. E. Ramirez,¹⁰⁸ A. Ramos-Buades,¹⁰⁶ Javed Rana,¹⁸ P. Rapagnani,^{100,35} V. Raymond,³⁶ M. Razzano,^{21,22} J. Read,²⁸ T. Regimbau,^{66,7} L. Rei,⁶¹ S. Reid,²⁶ D. H. Reitze,^{1,49} W. Ren,¹¹ F. Ricci,^{100,35} P. M. Ricker,¹¹ G. M. Riemenschneider,^{147,157} K. Riles,¹²³ M. Rizzo,⁵⁹ N. A. Robertson,^{1,45} R. Robie,⁴⁵ F. Robinet,²⁷ T. Robson,¹⁰⁵ A. Rocchi,³³ L. Rolland,⁷ J. G. Rollins,¹ V. J. Roma,⁷⁰ R. Romano,^{3,4} C. L. Romel,⁴⁶ J. H. Romie,⁶ D. Rosińska,^{158,55} M. P. Ross,¹⁵⁹ S. Rowan,⁴⁵ A. Rüdiger,^{9,10} P. Ruggi,³⁰ G. Rutins,¹⁶⁰ K. Ryan,⁴⁶ S. Sachdev,¹ T. Sadecki,⁴⁶ M. Sakellariadou,¹⁶¹ L. Salconi,³⁰ M. Saleem,¹¹⁹ F. Salemi,⁹ A. Samajdar,^{149,13} L. Sammut,⁵ L. M. Sampson,⁹¹ E. J. Sanchez,¹ L. E. Sanchez,¹ N. Sanchis-Gual,²³ V. Sandberg,⁴⁶ J. R. Sanders,⁴³ N. Sarin,⁵ B. Sassolas,²⁵ B. S. Sathyaprakash,^{88,36} P. R. Saulson,⁴³ O. Sauter,¹²³ R. L. Savage,⁴⁶ A. Sawadsky,³⁴ P. Schale,⁷⁰ M. Scheel,⁴⁷ J. Scheuer,⁹¹ P. Schmidt,⁶⁵ R. Schnabel,³⁴ R. M. S. Schofield,⁷⁰ A. Schönbeck,³⁴ E. Schreiber,^{9,10} D. Schuette,^{9,10} B. W. Schulte,^{9,10} B. F. Schutz,^{36,9} S. G. Schwalbe,³⁷ J. Scott,⁴⁵ S. M. Scott,²⁴ E. Seidel,¹¹ D. Sellers,⁶ A. S. Sengupta,¹⁶² D. Sentenac,³⁰ V. Sequino,^{32,33,16} A. Sergeev,¹²⁹ Y. Setyawati,⁹ D. A. Shaddock,²⁴ T. J. Shaffer,⁴⁶ A. A. Shah,¹³⁹ M. S. Shahriar,⁹¹ M. B. Shaner,¹¹² L. Shao,³⁸ B. Shapiro,⁵⁰ P. Shawhan,⁷⁶ H. Shen,¹¹ D. H. Shoemaker,¹⁴ D. M. Shoemaker,⁷⁷ K. Siellez,⁷⁷ X. Siemens,²⁰ M. Sieniawska,⁵⁵ D. Sigg,⁴⁶ A. D. Silva,¹⁵ L. P. Singer,⁸⁰ A. Singh,^{9,10} A. Singhal,^{16,35} A. M. Sintes,¹⁰⁶ B. J. J. Slagmolen,²⁴ T. J. Slaven-Blair,⁶⁴ B. Smith,⁶ J. R. Smith,²⁸ R. J. E. Smith,⁵ S. Somala,¹⁶³ E. J. Son,¹³² B. Sorazu,⁴⁵ F. Sorrentino,⁶¹ T. Souradeep,¹⁸ A. P. Spencer,⁴⁵ A. K. Srivastava,¹¹⁰ K. Staats,³⁷ M. Steinke,^{9,10} J. Steinlechner,^{34,45} S. Steinlechner,³⁴ D. Steinmeyer,^{9,10} B. Steltner,^{9,10} S. P. Stevenson,¹⁵⁶ D. Stocks,⁵⁰ R. Stone,¹⁰⁸ D. J. Stops,⁶⁰ K. A. Strain,⁴⁵ G. Stratta,^{72,73} S. E. Strigin,⁶³ A. Strunk,⁴⁶ R. Sturani,¹⁶⁴ A. L. Stuver,¹⁶⁵ T. Z. Summerscales,¹⁶⁶ L. Sun,⁹⁹ S. Sunil,¹¹⁰ J. Suresh,¹⁸ P. J. Sutton,³⁶ B. L. Swinkels,¹³ M. J. Szczepańczyk,³⁷ M. Tacca,¹³ S. C. Tait,⁴⁵ C. Talbot,⁵ D. Talukder,⁷⁰ D. B. Tanner,⁴⁹ M. Tápai,¹²⁰ A. Taracchini,³⁸ J. D. Tasson,⁹⁵ J. A. Taylor,¹³⁹ R. Taylor,¹ S. V. Tewari,¹⁵³ T. Theeg,^{9,10} F. Thies,^{9,10} E. G. Thomas,⁶⁰ M. Thomas,⁶ P. Thomas,⁴⁶ K. A. Thorne,⁶ E. Thrane,⁵ S. Tiwari,^{16,98} V. Tiwari,³⁶ K. V. Tokmakov,²⁶ K. Toland,⁴⁵ M. Tonelli,^{21,22} Z. Tornasi,⁴⁵ A. Torres-Forné,²³ C. I. Torrie,¹ D. Töyrä,⁶⁰ F. Travasso,^{30,42} G. Traylor,⁶ J. Trinastic,⁴⁹ M. C. Tringali,^{113,98} A. Trovato,²⁹ L. Trozzo,^{167,22} K. W. Tsang,¹³ M. Tse,¹⁴ R. Tso,⁴⁷ D. Tsuna,⁸² L. Tsukada,⁸² D. Tuyenbayev,¹⁰⁸ K. Ueno,²⁰ D. Ugolini,¹⁶⁸ A. L. Urban,¹ S. A. Usman,³⁶ H. Vahlbruch,^{9,10} G. Vajente,¹ G. Valdes,² N. van Bakel,¹³ M. van Beuzekom,¹³ J. F. J. van den Brand,^{75,13} C. Van Den Broeck,^{13,169} D. C. Vander-Hyde,⁴³ L. van der Schaaf,¹³ J. V. van Heijningen,¹³ A. A. van Veggel,⁴⁵ M. Vardaro,^{52,53} V. Varma,⁴⁷ S. Vass,¹ M. Vasúth,⁴⁸ A. Vecchio,⁶⁰ G. Vedovato,⁵³ J. Veitch,⁴⁵ P. J. Veitch,⁵⁶ K. Venkateswara,¹⁵⁹ G. Venugopalan,¹ D. Verkindt,⁷ F. Vetrano,^{72,73} A. Viceré,^{72,73} A. D. Viets,²⁰ S. Vinciguerra,⁶⁰ D. J. Vine,¹⁶⁰ J.-Y. Vinet,⁶⁶ S. Vitale,¹⁴ T. Vo,⁴³ H. Vocca,^{41,42} C. Vorvick,⁴⁶ S. P. Vyatchanin,⁶³ A. R. Wade,¹ L. E. Wade,⁸⁵ M. Wade,⁸⁵ R. Walet,¹³ M. Walker,²⁸ L. Wallace,¹ S. Walsh,^{20,9} G. Wang,^{16,22} H. Wang,⁶⁰ J. Z. Wang,¹²³ W. H. Wang,¹⁰⁸ Y. F. Wang,⁹⁶ R. L. Ward,²⁴ J. Warner,⁴⁶ M. Was,⁷ J. Watchi,¹⁰¹ B. Weaver,⁴⁶ L.-W. Wei,^{9,10} M. Weinert,^{9,10} A. J. Weinstein,¹ R. Weiss,¹⁴ F. Wellmann,^{9,10} L. Wen,⁶⁴ E. K. Wessel,¹¹ P. Weßels,^{9,10} J. Westerweck,⁹ K. Wette,²⁴ J. T. Whelan,⁵⁹ B. F. Whiting,⁴⁹ C. Whittle,¹⁴ D. Wilken,^{9,10} D. Williams,⁴⁵ R. D. Williams,¹ A. R. Williamson,^{59,65} J. L. Willis,^{1,124} B. Willke,^{9,10} M. H. Wimmer,^{9,10} W. Winkler,^{9,10} C. C. Wipf,¹ H. Wittel,^{9,10} G. Woan,⁴⁵ J. Woehler,^{9,10} J. K. Wofford,⁵⁹ W. K. Wong,⁹⁶ J. Worden,⁴⁶ J. L. Wright,⁴⁵ D. S. Wu,^{9,10} D. M. Wysocki,⁵⁹ S. Xiao,¹ W. Yam,¹⁴ H. Yamamoto,¹ C. C. Yancey,⁷⁶ L. Yang,¹⁷⁰ M. J. Yap,²⁴ M. Yazback,⁴⁹ Hang Yu,¹⁴ Haocun Yu,¹⁴ M. Yvert,⁷ A. Zadrożny,¹³⁴ M. Zanolin,³⁷ T. Zelenova,³⁰ J.-P. Zendri,⁵³ M. Zevin,⁹¹ J. Zhang,⁶⁴ L. Zhang,¹ M. Zhang,¹⁴⁴ T. Zhang,⁴⁵ Y.-H. Zhang,^{9,10} C. Zhao,⁶⁴ M. Zhou,⁹¹ Z. Zhou,⁹¹ S. J. Zhu,^{9,10} X. J. Zhu,⁵ A. B. Zimmerman,⁹² Y. Zlochower,⁵⁹ M. E. Zucker,^{1,14} and J. Zweizig¹

(The LIGO Scientific Collaboration and the Virgo Collaboration)

- ¹LIGO, California Institute of Technology, Pasadena, CA 91125, USA
- ²Louisiana State University, Baton Rouge, LA 70803, USA
- ³Università di Salerno, Fisciano, I-84084 Salerno, Italy
- ⁴INFN, Sezione di Napoli, Complesso Universitario di Monte S. Angelo, I-80126 Napoli, Italy
- ⁵OzGrav, School of Physics & Astronomy, Monash University, Clayton 3800, Victoria, Australia
- ⁶LIGO Livingston Observatory, Livingston, LA 70754, USA
- ⁷Laboratoire d'Annecy de Physique des Particules (LAPP), Univ. Grenoble Alpes, Université Savoie Mont Blanc, CNRS/IN2P3, F-74941 Annecy, France
- ⁸University of Sannio at Benevento, I-82100 Benevento, Italy and INFN, Sezione di Napoli, I-80100 Napoli, Italy
- ⁹Max Planck Institute for Gravitational Physics (Albert Einstein Institute), D-30167 Hannover, Germany
- ¹⁰Leibniz Universität Hannover, D-30167 Hannover, Germany
- ¹¹NCSA, University of Illinois at Urbana-Champaign, Urbana, IL 61801, USA
- ¹²University of Cambridge, Cambridge CB2 1TN, United Kingdom
- ¹³Nikhef, Science Park 105, 1098 XG Amsterdam, The Netherlands
- ¹⁴LIGO, Massachusetts Institute of Technology, Cambridge, MA 02139, USA
- ¹⁵Instituto Nacional de Pesquisas Espaciais, 12227-010 São José dos Campos, São Paulo, Brazil
- ¹⁶Gran Sasso Science Institute (GSSI), I-67100 L'Aquila, Italy
- ¹⁷INFN, Laboratori Nazionali del Gran Sasso, I-67100 Assergi, Italy
- ¹⁸Inter-University Centre for Astronomy and Astrophysics, Pune 411007, India
- ¹⁹International Centre for Theoretical Sciences, Tata Institute of Fundamental Research, Bengaluru 560089, India
- ²⁰University of Wisconsin-Milwaukee, Milwaukee, WI 53201, USA
- ²¹Università di Pisa, I-56127 Pisa, Italy
- ²²INFN, Sezione di Pisa, I-56127 Pisa, Italy
- ²³Departamento de Astronomía y Astrofísica, Universitat de València, E-46100 Burjassot, València, Spain
- ²⁴OzGrav, Australian National University, Canberra, Australian Capital Territory 0200, Australia
- ²⁵Laboratoire des Matériaux Avancés (LMA), CNRS/IN2P3, F-69622 Villeurbanne, France
- ²⁶SUPA, University of Strathclyde, Glasgow G1 1XQ, United Kingdom
- ²⁷LAL, Univ. Paris-Sud, CNRS/IN2P3, Université Paris-Saclay, F-91898 Orsay, France
- ²⁸California State University Fullerton, Fullerton, CA 92831, USA
- ²⁹APC, AstroParticule et Cosmologie, Université Paris Diderot, CNRS/IN2P3, CEA/Irfu, Observatoire de Paris, Sorbonne Paris Cité, F-75205 Paris Cedex 13, France
- ³⁰European Gravitational Observatory (EGO), I-56021 Cascina, Pisa, Italy
- ³¹Chennai Mathematical Institute, Chennai 603103, India
- ³²Università di Roma Tor Vergata, I-00133 Roma, Italy
- ³³INFN, Sezione di Roma Tor Vergata, I-00133 Roma, Italy
- ³⁴Universität Hamburg, D-22761 Hamburg, Germany
- ³⁵INFN, Sezione di Roma, I-00185 Roma, Italy
- ³⁶Cardiff University, Cardiff CF24 3AA, United Kingdom
- ³⁷Embry-Riddle Aeronautical University, Prescott, AZ 86301, USA
- ³⁸Max Planck Institute for Gravitational Physics (Albert Einstein Institute), D-14476 Potsdam-Golm, Germany
- ³⁹Korea Institute of Science and Technology Information, Daejeon 34141, Korea
- ⁴⁰West Virginia University, Morgantown, WV 26506, USA
- ⁴¹Università di Perugia, I-06123 Perugia, Italy
- ⁴²INFN, Sezione di Perugia, I-06123 Perugia, Italy
- ⁴³Syracuse University, Syracuse, NY 13244, USA
- ⁴⁴University of Minnesota, Minneapolis, MN 55455, USA
- ⁴⁵SUPA, University of Glasgow, Glasgow G12 8QQ, United Kingdom
- ⁴⁶LIGO Hanford Observatory, Richland, WA 99352, USA
- ⁴⁷Caltech CaRT, Pasadena, CA 91125, USA
- ⁴⁸Wigner RCP, RMKI, H-1121 Budapest, Konkoly Thege Miklós út 29-33, Hungary
- ⁴⁹University of Florida, Gainesville, FL 32611, USA
- ⁵⁰Stanford University, Stanford, CA 94305, USA
- ⁵¹Università di Camerino, Dipartimento di Fisica, I-62032 Camerino, Italy
- ⁵²Università di Padova, Dipartimento di Fisica e Astronomia, I-35131 Padova, Italy
- ⁵³INFN, Sezione di Padova, I-35131 Padova, Italy
- ⁵⁴MTA-ELTE Astrophysics Research Group, Institute of Physics, Eötvös University, Budapest 1117, Hungary
- ⁵⁵Nicolaus Copernicus Astronomical Center, Polish Academy of Sciences, 00-716, Warsaw, Poland
- ⁵⁶OzGrav, University of Adelaide, Adelaide, South Australia 5005, Australia
- ⁵⁷Dipartimento di Scienze Matematiche, Fisiche e Informatiche, Università di Parma, I-43124 Parma, Italy
- ⁵⁸INFN, Sezione di Milano Bicocca, Gruppo Collegato di Parma, I-43124 Parma, Italy

- ⁵⁹Rochester Institute of Technology, Rochester, NY 14623, USA
- ⁶⁰University of Birmingham, Birmingham B15 2TT, United Kingdom
- ⁶¹INFN, Sezione di Genova, I-16146 Genova, Italy
- ⁶²RRCAT, Indore, Madhya Pradesh 452013, India
- ⁶³Faculty of Physics, Lomonosov Moscow State University, Moscow 119991, Russia
- ⁶⁴OzGrav, University of Western Australia, Crawley, Western Australia 6009, Australia
- ⁶⁵Department of Astrophysics/IMAPP, Radboud University Nijmegen, P.O. Box 9010, 6500 GL Nijmegen, The Netherlands
- ⁶⁶Artemis, Université Côte d'Azur, Observatoire Côte d'Azur, CNRS, CS 34229, F-06304 Nice Cedex 4, France
- ⁶⁷Physik-Institut, University of Zurich, Winterthurerstrasse 190, 8057 Zurich, Switzerland
- ⁶⁸Univ Rennes, CNRS, Institut FOTON - UMR6082, F-3500 Rennes, France
- ⁶⁹Washington State University, Pullman, WA 99164, USA
- ⁷⁰University of Oregon, Eugene, OR 97403, USA
- ⁷¹Laboratoire Kastler Brossel, Sorbonne Université, CNRS, ENS-Université PSL, Collège de France, F-75005 Paris, France
- ⁷²Università degli Studi di Urbino 'Carlo Bo,' I-61029 Urbino, Italy
- ⁷³INFN, Sezione di Firenze, I-50019 Sesto Fiorentino, Firenze, Italy
- ⁷⁴Astronomical Observatory Warsaw University, 00-478 Warsaw, Poland
- ⁷⁵VU University Amsterdam, 1081 HV Amsterdam, The Netherlands
- ⁷⁶University of Maryland, College Park, MD 20742, USA
- ⁷⁷School of Physics, Georgia Institute of Technology, Atlanta, GA 30332, USA
- ⁷⁸Université Claude Bernard Lyon 1, F-69622 Villeurbanne, France
- ⁷⁹Università di Napoli 'Federico II,' Complesso Universitario di Monte S. Angelo, I-80126 Napoli, Italy
- ⁸⁰NASA Goddard Space Flight Center, Greenbelt, MD 20771, USA
- ⁸¹Dipartimento di Fisica, Università degli Studi di Genova, I-16146 Genova, Italy
- ⁸²RESCEU, University of Tokyo, Tokyo, 113-0033, Japan.
- ⁸³Tsinghua University, Beijing 100084, China
- ⁸⁴Texas Tech University, Lubbock, TX 79409, USA
- ⁸⁵Kenyon College, Gambier, OH 43022, USA
- ⁸⁶The University of Mississippi, University, MS 38677, USA
- ⁸⁷Museo Storico della Fisica e Centro Studi e Ricerche "Enrico Fermi", I-00184 Roma, Italyrico Fermi, I-00184 Roma, Italy
- ⁸⁸The Pennsylvania State University, University Park, PA 16802, USA
- ⁸⁹National Tsing Hua University, Hsinchu City, 30013 Taiwan, Republic of China
- ⁹⁰Charles Sturt University, Wagga Wagga, New South Wales 2678, Australia
- ⁹¹Center for Interdisciplinary Exploration & Research in Astrophysics (CIERA), Northwestern University, Evanston, IL 60208, USA
- ⁹²Canadian Institute for Theoretical Astrophysics, University of Toronto, Toronto, Ontario M5S 3H8, Canada
- ⁹³University of Chicago, Chicago, IL 60637, USA
- ⁹⁴Pusan National University, Busan 46241, Korea
- ⁹⁵Carleton College, Northfield, MN 55057, USA
- ⁹⁶The Chinese University of Hong Kong, Shatin, NT, Hong Kong
- ⁹⁷INAF, Osservatorio Astronomico di Padova, I-35122 Padova, Italy
- ⁹⁸INFN, Trento Institute for Fundamental Physics and Applications, I-38123 Povo, Trento, Italy
- ⁹⁹OzGrav, University of Melbourne, Parkville, Victoria 3010, Australia
- ¹⁰⁰Università di Roma 'La Sapienza,' I-00185 Roma, Italy
- ¹⁰¹Université Libre de Bruxelles, Brussels 1050, Belgium
- ¹⁰²Sonoma State University, Rohnert Park, CA 94928, USA
- ¹⁰³Departamento de Matemáticas, Universitat de València, E-46100 Burjassot, València, Spain
- ¹⁰⁴Columbia University, New York, NY 10027, USA
- ¹⁰⁵Montana State University, Bozeman, MT 59717, USA
- ¹⁰⁶Universitat de les Illes Balears, IAC3—IEEC, E-07122 Palma de Mallorca, Spain
- ¹⁰⁷University of Rhode Island, Kingston, RI 02881, USA
- ¹⁰⁸The University of Texas Rio Grande Valley, Brownsville, TX 78520, USA
- ¹⁰⁹Bellevue College, Bellevue, WA 98007, USA
- ¹¹⁰Institute for Plasma Research, Bhat, Gandhinagar 382428, India
- ¹¹¹The University of Sheffield, Sheffield S10 2TN, United Kingdom
- ¹¹²California State University, Los Angeles, 5151 State University Dr, Los Angeles, CA 90032, USA
- ¹¹³Università di Trento, Dipartimento di Fisica, I-38123 Povo, Trento, Italy
- ¹¹⁴Montclair State University, Montclair, NJ 07043, USA
- ¹¹⁵National Astronomical Observatory of Japan, 2-21-1 Osawa, Mitaka, Tokyo 181-8588, Japan
- ¹¹⁶Observatori Astronòmic, Universitat de València, E-46980 Paterna, València, Spain

- ¹¹⁷*School of Mathematics, University of Edinburgh, Edinburgh EH9 3FD, United Kingdom*
- ¹¹⁸*University and Institute of Advanced Research, Koba Institutional Area, Gandhinagar Gujarat 382007, India*
- ¹¹⁹*Indian Institute of Technology Bombay, Powai, Mumbai 400 076, India*
- ¹²⁰*University of Szeged, Dóm tér 9, Szeged 6720, Hungary*
- ¹²¹*Tata Institute of Fundamental Research, Mumbai 400005, India*
- ¹²²*INAF, Osservatorio Astronomico di Capodimonte, I-80131, Napoli, Italy*
- ¹²³*University of Michigan, Ann Arbor, MI 48109, USA*
- ¹²⁴*Abilene Christian University, Abilene, TX 79699, USA*
- ¹²⁵*American University, Washington, D.C. 20016, USA*
- ¹²⁶*University of Southampton, Southampton SO17 1BJ, United Kingdom*
- ¹²⁷*University of Białystok, 15-424 Białystok, Poland*
- ¹²⁸*University of Washington Bothell, 18115 Campus Way NE, Bothell, WA 98011, USA*
- ¹²⁹*Institute of Applied Physics, Nizhny Novgorod, 603950, Russia*
- ¹³⁰*Korea Astronomy and Space Science Institute, Daejeon 34055, Korea*
- ¹³¹*Inje University Gimhae, South Gyeongsang 50834, Korea*
- ¹³²*National Institute for Mathematical Sciences, Daejeon 34047, Korea*
- ¹³³*Ulsan National Institute of Science and Technology, Ulsan 44919, South Korea*
- ¹³⁴*NCBJ, 05-400 Świerk-Otwock, Poland*
- ¹³⁵*Institute of Mathematics, Polish Academy of Sciences, 00656 Warsaw, Poland*
- ¹³⁶*Cornell University, Ithaca, NY 14850, USA*
- ¹³⁷*Hillsdale College, Hillsdale, MI 49242, USA*
- ¹³⁸*Hanyang University, Seoul 04763, Korea*
- ¹³⁹*NASA Marshall Space Flight Center, Huntsville, AL 35811, USA*
- ¹⁴⁰*Dipartimento di Fisica, Università degli Studi Roma Tre, I-00154 Roma, Italy*
- ¹⁴¹*INFN, Sezione di Roma Tre, I-00154 Roma, Italy*
- ¹⁴²*ESPCI, CNRS, F-75005 Paris, France*
- ¹⁴³*Southern University and A&M College, Baton Rouge, LA 70813, USA*
- ¹⁴⁴*College of William and Mary, Williamsburg, VA 23187, USA*
- ¹⁴⁵*Centre Scientifique de Monaco, 8 quai Antoine 1er, MC-98000, Monaco*
- ¹⁴⁶*Indian Institute of Technology Madras, Chennai 600036, India*
- ¹⁴⁷*INFN Sezione di Torino, Via P. Giuria 1, I-10125 Torino, Italy*
- ¹⁴⁸*Institut des Hautes Etudes Scientifiques, F-91440 Bures-sur-Yvette, France*
- ¹⁴⁹*IISER-Kolkata, Mohanpur, West Bengal 741252, India*
- ¹⁵⁰*Whitman College, 345 Boyer Avenue, Walla Walla, WA 99362 USA*
- ¹⁵¹*Scuola Normale Superiore, Piazza dei Cavalieri 7, I-56126 Pisa, Italy*
- ¹⁵²*Université de Lyon, F-69361 Lyon, France*
- ¹⁵³*Hobart and William Smith Colleges, Geneva, NY 14456, USA*
- ¹⁵⁴*INFN, Sezione di Milano Bicocca, I-20126, Milano, Italy*
- ¹⁵⁵*Università degli Studi di Firenze, I-50121 Firenze, Italy*
- ¹⁵⁶*OzGrav, Swinburne University of Technology, Hawthorn VIC 3122, Australia*
- ¹⁵⁷*Dipartimento di Fisica, Università di Torino, Via P. Giuria 1, I-10125 Torino, Italy*
- ¹⁵⁸*Janusz Gil Institute of Astronomy, University of Zielona Góra, 65-265 Zielona Góra, Poland*
- ¹⁵⁹*University of Washington, Seattle, WA 98195, USA*
- ¹⁶⁰*SUPA, University of the West of Scotland, Paisley PA1 2BE, United Kingdom*
- ¹⁶¹*King's College London, University of London, London WC2R 2LS, United Kingdom*
- ¹⁶²*Indian Institute of Technology Hyderabad, Sangareddy, Khandi, Telangana 502285, India*
- ¹⁶³*Indian Institute of Technology Hyderabad, Sangareddy, Khandi, Telangana 502285, India*
- ¹⁶⁴*International Institute of Physics, Universidade Federal do Rio Grande do Norte, Natal RN 59078-970, Brazil*
- ¹⁶⁵*Villanova University, 800 Lancaster Ave, Villanova, PA 19085, USA*
- ¹⁶⁶*Andrews University, Berrien Springs, MI 49104, USA*
- ¹⁶⁷*Università di Siena, I-53100 Siena, Italy*
- ¹⁶⁸*Trinity University, San Antonio, TX 78212, USA*
- ¹⁶⁹*Van Swinderen Institute for Particle Physics and Gravity, University of Groningen, Nijenborgh 4, 9747 AG Groningen, The Netherlands*
- ¹⁷⁰*Colorado State University, Fort Collins, CO 80523, USA*